REPORT DOCUMENTATION PAGE

Form Approved
OMB NO. 0704-0188

1. AGENCY USE ONLY (Leave Blank)	2. REPORT DATE	3. REPORT TYPE AND DATES COVERED
	April, 2004	Final Report

4. TITLE AND SUBTITLE
Damage Models and Computational Tools for Health-Monitoring of Smart Structures

5. FUNDING NUMBERS
DAAD 19-01-1-0483

6. AUTHOR(S)
J. N. Reddy

7. PERFORMING ORGANIZATION NAME(S) AND ADDRESS(ES)
Department of Mechanical Engineering,
Texas A&M University
College Station, Texas 77843-3123

9. SPONSORING / MONITORING AGENCY NAME(S) AND ADDRESS(ES)
U. S. Army Research Office
P.O. Box 12211
Research Triangle Park, NC 27709-2211

10. SPONSORING / MONITORING AGENCY REPORT NUMBER
41551.5-EG

11. SUPPLEMENTARY NOTES
The views, opinions and/or findings contained in this report are those of the author(s) and should not be construed as an official Department of the Army position, policy or decision, unless so designated by the documentation.

12 a. DISTRIBUTION / AVAILABILITY STATEMENT
Approved for public Release; Availability unlimited

12 b. DISTRIBUTION CODE

13. ABSTRACT (Maximum 200 words)
The primary goal of this research was to develop physically based damage models, computational approaches based on shear deformation plate theories and layerwise theory, a finite element formulation for the analysis of thin and thick laminated composite structures with embedded sensors/actuators. During the period of this project the following tasks have been completed: (1) literature search to assess damage and failures models; (2) theoretical formulation of the layerwise models for smart composite structures, (3) formulation of damage models, (4) finite element analysis of laminated adaptive plate structures using the layerwise theory, and (5) finite element analysis of laminated adaptive plate structures using the single-layer theories (classical, first-order, and third-order plate theories). Geometric nonlinearities are accounted for and parametric effects of lamination schemes, material properties, and boundary conditions were investigated.

14. SUBJECT TERMS
laminated composite plates, finite element models, layerwise theory, magnetostrictive materials, smart structures, third-order theory, transient response

15. NUMBER OF PAGES
42 including cover page

16. PRICE CODE

17. SECURITY CLASSIFICATION OR REPORT	18. SECURITY CLASSIFICATION ON THIS PAGE	19. SECURITY CLASSIFICATION OF ABSTRACT	20. LIMITATION OF ABSTRACT
UNCLASSIFIED	UNCLASSIFIED	UNCLASSIFIED	UL

REPORT DOCUMENTATION PAGE (SF298)
(Continuation Sheet)

1. LIST OF MANUSCRIPTS

S. J. Lee and **J. N. Reddy**, ``Nonlinear Deflection Control of Laminated Plates Using Third-Order Shear Deformation Theory," *Int. J. Mechanics & Materials in Design,* to appear.

S. J. Lee and **J. N. Reddy**, ``Vibration Suppression of Laminated Shells by Higher-Order Shear Deformation Theory," *Int. J. Engineering Science,* in review

W. Aliaga and **J. N. Reddy**, "Nonlinear Thermoelastic Response of Functionally Graded Plates Using the Third-Order Plate Theory," *International Journal of Computational Engineering Science* (to appear).

M. C. Ray and **J. N. Reddy**, "Effect of Delamination on the Active Constrained Layer Damping of Laminated Composite Beams," *AIAA Journal* (to appear).

J. E. Semedo Garção, C. M. Mota Soares, C. A. Mota Soares and **J. N. Reddy** ``Analysis of Laminated Adaptative Structures Using Layerwise Finite Element Models" *Computers and Structures*, to appear.

M. C. Ray and **J. N. Reddy**, "Optimal Control of Thin Circular Cylindrical Laminated Composite Shells Using Active Constrained Layer Damping Treatment," *Smart Materials and Structures*, Vol. 13, pp. 64-72, 2004.

S. J. Lee, **J. N. Reddy**, and F. Rostam-Abadi, "Transient Analysis of Laminated Composite Plates with Embedded Smart Material Layers," *Finite Elements in Analysis and Design.*, Vol. 40, Nos. 5-6, pp. 463—484, 2004.

2. SCIENTIFIC PERSONNEL and HONORS AND AWARDS

- J. N. Reddy, Z.-Q. Cheng, A. W. Aliaga, S. J. Lee
- J. N. Reddy was invited as a key note speaker to *Smart Materials, Structures and Systems*, 12-15 Dec 2002, Bangalore, INDIA).
- J. N., Reddy, *Texas A&M Bush Excellence Award for Faculty in International Research* award, 2003.
- J. N., Reddy, *Distinguished Achievement in Teaching* Award, Association of Former Students (AFS), Texas A&M University, 2002.
- J. N., Reddy, *Computational Solid Mechanics* award of the US Association for Computational Mechanics, July 2003.
- J. N., Reddy, *Fellow* of the American Society of Composites (ASC), October 2002.

3. INVENTIONS None

4. SCIENTIFIC PROGRESS AND ACCOMPLISHMENTS

The primary goal of this research was to develop physically based damage models, computational approaches based on shear deformation plate theories and layerwise theory, a finite element formulation for the analysis of thin and thick laminated composite structures with embedded sensors/actuators. During the period of this project the following tasks have been completed: (1) literature search to assess damage and failures models; (2) theoretical formulation of the layerwise models for smart composite structures, (3) formulation of damage models, (4) finite element analysis of laminated adaptive plate structures using the layerwise theory, and (5) finite element analysis of laminated adaptive plate structures using the single-layer theories (classical, first-order, and third-order plate theories). Geometric nonlinearities are accounted for and parametric effects of lamination schemes, material properties, and boundary conditions were investigated.

5. TECHNOLOGY TRANSFER

Interacted with Mr. Farzad Rostam-Abadi of U.S. Army Tank-Automotive Tank and Armaments Command (TACOM), AMSTA-TR-R, Warren, Michigan 48397.

Damage Models and Computational Tools for Health-Monitoring of Smart Structures

J. N. Reddy
Department of Mechanical Engineering,
Texas A&M University
College Station, Texas 77843-3123
Tel: (979) 690-7153
E-mail: jnreddy@tamu.edu

Grant No. DAAD 19-01-1-0483

Final Technical Report submitted to

U. S. Army Research Office
P.O. Box 12211
Research Triangle Park, NC 27709-2211

April 2004

DAMAGE MODELS AND COMPUTATIONAL TOOLS FOR HEALTH MONITORING OF SMAT STUCTURES

by

J. N. Reddy
Department of Mechanical Engineering,
Texas A&M University
College Station, Texas 77843-3123
Tel: (979) 690-7153
E-mail: jnreddy@tamu.edu

EXECUTIVE SUMMARY

The primary goal of this research was to develop physically based damage models, computational approaches based on shear deformation plate theories and layerwise theory, a finite element formulation for the analysis of thin and thick laminated composite structures with embedded sensors/actuators. During the period of this project the following tasks have been completed: (1) literature search to assess damage and failures models; (2) theoretical formulation of the layerwise models for smart composite structures, (3) formulation of damage models, (4) finite element analysis of laminated adaptive plate structures using the layerwise theory, and (5) finite element analysis of laminated adaptive plate structures using the single-layer theories (classical, first-order, and third-order plate theories). Geometric nonlinearities are accounted for and parametric effects of lamination schemes, material properties, and boundary conditions were investigated.

TECHNICAL DISCUSSION

1. Damage Models

1.1 *Introduction*

Fiber-reinforced laminated composites typically exhibit several different forms of progressive damage including fiber breakage, fiber buckling, fiber/matrix debonding, matrix cracking, individual ply rupture and separation between adjacent plies (i.e. delamination.) These modes of damage are often initiated at loads that are far below the ultimate failure load of a composite material. Any damage that is initiated tends to progress as the loading is further increased or cycled, and thus effectively degrades the stiffness of the material, causing significant load redistribution before ultimate failure occurs. To capture this complex behavior in a finite element simulation, two different approaches have emerged for the development of damage-dependent constitutive relations: a phenomenological approach (known as *continuum damage mechanics*, or CDM), and a micromechanics approach. In practice, the difference between these two approaches is often blurred; however, in the extreme case, we can differentiate between the two approaches as follows.

- The CDM approach attempts to predict damage accumulation and stiffness reduction in the *equivalent* homogenized version of the heterogeneous material.
- The micromechanics approach attempts to predict damage accumulation and stiffness reduction in the heterogeneous material before homogenization.

Therefore we can say that the difference between the two approaches is simply a matter of the timing of the homogenization process. The micromechanics approach has the potential for greater accuracy; however, it typically involves significantly more computational effort and also requires more experimentally derived material data (much of which is often unavailable). Given these obstacles, "from a practical point of view, it is difficult to imagine that a purely micromechanical theory, with all of its complexities, will ever replace a properly formulated phenomenological theory as a design tool," (Krajcinovic [1,2]). Perhaps in its most useful sense, the micromechanics-based damage model can be utilized as a basis on which a simplified CDM model can be built with a reasonable chance of replicating experimentally observed trends over a wide spectrum of materials and responses (Krajcinovic [1,2]). This is essentially the same philosophy adopted in the current proposal for a general-purpose finite element framework capable of accurately and efficiently simulating the progressive damage of smart composites.

1.2 *Literature Review*

A detailed literature review of the existing damage and failure models was included in the first interim progress report. Here we briefly discuss the main developments of that review.

Chang and Chang [3] gave a progressive damage model for laminated composites containing stress concentrations and subjected to tensile loading. The aim was to assess damage and predict ultimate tensile strength. Stress and strain analysis was based on classical laminate theory, with material non-linearity also being considered. For matrix cracking failure, they proposed a matrix failure criterion. Fiber-matrix shearing and fiber breakage were predicted by a modified Yamada-Sun failure criterion. A property degradation model was also proposed. Results obtained from a nonlinear finite element model for laminates containing a circular hole were compared with experimental data.

Aboudi [4] presented a model in which the effect of damage due to imperfect bonding between constituents of composite materials was incorporated. The interface de-cohesion was described by two parameters which completely determine the degree of adhesion at the interfaces in the normal and tangential directions. Perfect bonding, perfect lubrication and complete debonding were obtained as special cases. The model also predicts the overall modulii and overall coefficients of thermal expansion of composites in the presence of imperfect bonding. Ladeveze and Le Dantec [5] presented a model of the mechanical behavior of an elementary ply in a fibrous composite laminate. Continuum damage mechanics theory was used to describe matrix microcracking and fiber-matrix debonding. To model the anelastic strains induced by damage, a plasticity model was proposed. The model takes into account the differences between tension and compression in the fiber direction. The model leads to a laminate failure criterion.

Homogenization approaches to damage have also been developed. These often involved a two-step process in two different ways: a) homogenization of the stationary (non-evolving) microstructure, i.e. fibers and matrix, followed by incorporation of the evolving damage as internal variables, and b) incorporation of damage in each phase followed by homogenization of the phases. Fish et al. [6] choose to carry out the two steps simultaneously by using an extended homogenization procedure, wherein the field variables and a damage variable are given asymptotic expansions. The micro level total displacement is assumed to have contributions from the elastic strain and a damage induced strain, d, which is related to the damage variable ω. The microstructure of a composite material is assumed to be locally periodic and the influence of this periodicity scale is assumed to be the same for both strains. To avoid a computational stability problem observed previously in local approaches, Fish et al. defined a non-local damage variable that is a weighted average over the two phases in a characteristic volume. Finally, they expressed damage evolution in each phase separately in terms of the damage energy release rates. Another example of the homogenization approach is

that of Ghosh and his colleagues [7-9]. These authors do not use the concept of damage as an internal variable; instead, they determine the damage events explicitly by local stress analysis and failure criteria. They also allow for non-uniformity in the distribution of one phase (particles or fibers) into another (matrix), and use Voronoi cells to represent this heterogeneity. The micro scale model is analyzed using the effective strain from the global (structure) scale results and the effective (average) modulus tensor is evaluated. When damage evolves, the two-scale analysis must be conducted iteratively.

One of primary difficulties that one faces in attempting to model progressive damage in fiber-reinforced laminated composites is that many of the damage modes (e.g. fiber breakage, fiber buckling, fiber/matrix debonding, matrix cracking) occur on geometric scales that are impractical to reach with direct mesh refinement. However, these forms of damage have a very significant effect on the stiffness of the heterogeneous material that constitutes the typical finite element. On the other hand, some forms of damage (e.g. ply rupture and delamination) occur on geometric scales that might be smaller or larger than the typical finite element, depending on the level of mesh discretization. Furthermore, the criteria used to evaluate the onset and progression of damage invariably involves the stress, strain and/or energy of the material and these results are known to exhibit a strong dependence on mesh descritization. Therefore, in attempting to develop a computational model that incorporates all these various forms of damage, we must distinguish between *macroscopic damage* and *microscopic damage.* Within the context of modeling and simulation, we will distinguish between these two categories of damage on the basis of whether the damage entity is smaller or larger than the computational reference scale (i.e. the geometric scale of the individual finite element.) Thus, our choice of using the geometric scale of the individual finite element as the reference for distinguishing microscopic damage from macroscopic damage leads to the following interpretations:

- Modeling of *microscopic damage* does not explicitly require modification of the basic assumed kinematics of the model, but does require modification of the material properties to account for the damaged or weakened state of the material. Typically, microscopic damage is handled by using a homogenized description of the distribution, density and orientation of the microcracks and microvoids that occur in the immediate neighborhood of a Gaussian integration point within a finite element. For finite elements that are significantly larger than the fiber/matrix RVE, but not necessarily larger than the thickness of a single lamina, *microscopic damage* typically includes fiber breakage, fiber buckling, fiber/matrix debonding and matrix cracking.

- Modeling of *macroscopic damage* explicitly requires modification of the basic assumed kinematics of the model. This category of damage includes cracks or voids that are of the same order or larger than the representative finite element size. For finite elements that are smaller than the thickness of a single lamina, *macroscopic damage* might include ply rupture and delamination. However, for very large finite elements whose smallest dimension is equivalent to the laminate thickness, even these forms of damage might be treated as microscopic damage. Of course, the appearance of macroscopic damage is necessarily preceded by cumulative microscopic damage that coalesces into macroscopic damage. Therefore, a simulation that is capable of predicting the appearance and subsequent propagation of macroscopic damage must necessarily incorporate both a mechanism to alter the material properties based on homogenized microscopic damage and a mechanism to alter the assumed kinematics based on macroscopic cracks and voids.

From the above description, it is obvious that the classification of a particular form of damage as *microscopic damage* or *macroscopic damage* depends upon the specific type and quality of computational results that we seek. This is the most influential factor in our choice of a particular mathematical model and a particular finite element size. Thus it is imperative that a general-purpose computational tool should be *flexible* in its treatment of damage modeling at

different geometric scales. Ideally, the classification of different physical modes of damage as microscopic or macroscopic should be automatically based on the characteristic element length scale that is appropriate for the particular results sought. Thus for one type of problem, the simulation code might handle delamination as a macroscopic form of damage, while for another type of problem the code might handle delamination as a microscopic form of damage. While the complete satisfaction of this goal is impractical given the current state of simulation technology, the software development proposed in Phase II of this effort represents a significant step in this direction.

1.3 *Microscopic and macroscopic damage modeling*

The computational model for simulating progressive damage in smart composites incorporates the following mechanisms for modeling the initiation and propagation of damage induced by service loads.

1. *Microscopic damage* is modeled within the context of *Continuum Damage Mechanics*, or CDM, where the material properties are modified to account for the weakened state of the material due to the presence of distributed microcracks and microvoids that occur as a result of stress concentrations within the heterogeneous laminate. With the exception of pre-existing delaminations, all forms of damage are initially modeled as microscopic damage using continuum damage mechanics, regardless of the size of a particular finite element. This method is appropriate up to the point where the microscopic damage becomes severe enough to cause coalescence into macroscopic damage (i.e. delamination or ply rupture) whose dimension is approximately equal to the dimension of the finite element. The successful implementation of the modeling of *microscopic* damage via continuum damage mechanics requires the following components:

   A. *Damage Variable* – Choose an appropriate tensorial form for the internal variable that will be used to characterize the microscopic damage. This internal variable, known as the *damage tensor*, is responsible for describing the distribution, density, and orientation of microcracks and microvoids. Various forms of the damage tensor have been proposed in the literature, for example, scalars, vectors, 2nd order tensors, and 4th order tensors (Skrzypek and Ganczarski [10]). Depending on the anticipated complexity of the damage process, we should choose the simplest tensor that is capable of accurately describing the distribution, density, and orientation of microcracks and microvoids for the intended type of problem. For fiber-reinforced composite laminae, the simplest form of the damage tensor that is capable of accurately describing microscopic damage is a symmetric 2nd order tensor whose principal directions are assumed to coincide with the principal material directions, i.e. orthotropic damage (Barbero and De Vivo [11]).

   B. *Stiffness Reduction Scheme* – Define the effective homogenized material properties in terms of the current level of the damage variable, i.e. we must have a consistent means to modify the original homogenized material properties to reflect the weakened state of the material due to the presence of distributed microcracks and microvoids. This is accomplished by using various *equivalence* principles, e.g. the principle of elastic energy equivalence.

   C. *Damage Surface* – Define a damage threshold criterion, i.e. a multidimensional surface in the space of state variables that must be exceeded before any damage can be initiated, or before existing damage can progress. Thus the damage surface serves to separate non-damaging behavior from damage-inducing behavior.

D. *Damage Evolution* – Define the damage evolution equation. Assuming that the damage surface has been reached, we must express the rate of change of the damage tensor as a function of the remaining state variables.

2. *Macroscopic damage* in the form of delamination is modeled by hierarchically enriching the kinematics of the model to permit general relative motion between the newly created interlaminar surfaces. Thus the appearance of macroscopic damage involves an increase in the number of degrees of freedom of the model. The successful implementation of the modeling of *macroscopic* damage requires the following components:

   A. *Kinematic Enhancement* – Incorporate a hierarchical description of the displacement field that permits degrees of freedom to be added to the existing model to account for the relative motion of newly created interlaminar surfaces due to delamination. The use of a hierarchical displacement field facilitates automation of the process since the existing mesh does require alteration; we simply add incremental displacement degrees of freedom to the existing model (Robbins and Reddy [5,6]).

   B. *Delamination Criterion* – Define a criterion, based on the homogenized, microscopic damage variable to indicate initiation and further propagation of delamination.

A detailed description of modeling of microscopic and macroscopic damage will be given in the following sections.

1.4 *Continuum damage mechanics at the meso-scale (i.e. ply Level)*

In the sequel, the use of the term *damage* is understood to mean *microscopic damage* unless explicitly stated otherwise. Thus the term *damage* is intended to indicate the presence of microcracks and microvoids that are small compared to the geometric dimensions of a typical finite element and can thus be handled to sufficient accuracy via *continuum damage mechanics*, or CDM. In most practical analyses of composite materials, the typical dimensions of a finite element do not approach the geometric scale of the fiber/matrix RVE. Thus it can be safely assumed that cracks and voids that are small compared to the thickness of a single fiber-reinforced composite lamina will be treated as microscopic damage and handled via CDM. Thus damage in the form of fiber breakage, fiber/matrix debonding, and matrix cracking will be treated via homogenization at the meso-scale (or ply level). This is analogous to the process used to define equivalent anisotropic material properties at the meso-scale (or ply level) by homogenization of the heterogeneous material constituents. In contrast, the modeling of delamination most often requires treatment as a form of macroscopic damage that cannot be homogenized.

The meso-scale continuum damage mechanics model developed in this study is capable of utilizing the full 3-D stress and strain fields evaluated at the ply level. This model represents an extension of the 2-D continuum damage mechanics model of Barbero and DeVivo [11], where each individual lamina was assumed to be in a state of 2-D plane stress. In the present CDM approach, the fiber-reinforced composite material that constitutes an individual lamina is replaced with a non-heterogeneous orthotropic material. Prior to the appearance of any damage, the equivalent orthotropic material may be considered homogeneous within the lamina. However, once damage initiates, the orthotropic material properties vary with respect to position within the lamina since damage occurs locally within the lamina depending on the local state of the material.

1.5 *Description of damage (kinematics)*

A symmetric 2nd order *damage tensor* $\mathbf{D} = D_{ij}\mathbf{e}_i\mathbf{e}_j$ is chosen to describe the distribution, density and orientation of microcracks and microdefects within the homogenized lamina. When the damage tensor **D** is expressed in an arbitrary coordinate system, it is difficult to assign physical meaning to its individual components (i.e. the D_{ij}). However, when the damage tensor is expressed in its principal coordinate system, the eigenvalues of **D** (denoted D_1, D_2, and D_3) have a simple physical interpretation. The i^{th} eigenvalue D_i represents the fractional reduction in load carrying area on planes that are perpendicular to the i^{th} principal direction. Thus the use of a symmetric 2nd order damage tensor implies that the microscopic damage is orthotropic (i.e. a system of microcracks and microvoids that are oriented along three mutually perpendicular directions. This type of damage tensor is most often appropriate for fiber-reinforced composite laminae since the predominate modes of microscopic damage are fiber breakage, fiber buckling, fiber/matrix debonding, and matrix cracks that are oriented either parallel to the reinforcing fibers or perpendicular to the reinforcing fibers. Furthermore, this orderly arrangement of microcracks can be described to an acceptable level of accuracy by using a 2nd order damage tensor **D** whose principal directions are assumed to coincide with the principal material directions of the lamina (Barbero and DeVivo [11]).

Damage tensor expressed in Arbitrary Coordinate System — Damage tensor expressed in Principal Material Coordinate System

$$\begin{bmatrix} D_{11} & D_{12} & D_{13} \\ D_{21} & D_{22} & D_{23} \\ D_{31} & D_{32} & D_{33} \end{bmatrix} \rightarrow \begin{bmatrix} D_{11} & 0 & 0 \\ 0 & D_{22} & 0 \\ 0 & 0 & D_{33} \end{bmatrix} \text{ or } \begin{bmatrix} D_1 & 0 & 0 \\ 0 & D_2 & 0 \\ 0 & 0 & D_3 \end{bmatrix} \tag{1}$$

This is a particularly convenient assumption since it permits us to work directly with the physically meaningful eigenvalues of **D** in a coordinate system that we already know from the material description. The eigenvalues of the damage tensor must be in the range $0 \le D_i \le 1$, where $D_i = 0$ corresponds to the case of complete lack of microcracks that are normal to the i^{th} principal material direction, while $D_i = 1$ corresponds to the case of complete separation of the material across planes that are normal to the i^{th} principal material direction. In practical terms, the material becomes unstable and ruptures when the damage reaches a critical value that is most often considerably less than 1. Thus the practical ranges for the three eigenvalues of the damage tensor are expressed as

$$0 \le D_i \le D_i^{crit} \qquad i = 1,2,3\,, \tag{2}$$

where the values $D_i^{crit} < 1$ $(i = 1,2,3)$ are considered to be material properties indicative of the fracture toughness of the material in planes normal to the principal material axes.

Related to the damage tensor is the *integrity tensor* $\mathbf{\Omega} = \Omega_{ij}\mathbf{e}_i\mathbf{e}_j$ given by

$$\mathbf{\Omega}\cdot\mathbf{\Omega} \equiv \mathbf{I} - \mathbf{D}\,, \quad \text{or} \quad \mathbf{\Omega} = \sqrt{\mathbf{I} - \mathbf{D}} \rightarrow \Omega_i = \sqrt{1 - D_i} \;\; i=1,2,3, \tag{3}$$

where Ω_i and D_i are the eigenvalues of the integrity tensor and the damage tensor respectively. Thus, while the eigenvalues of the damage tensor **D** provide a measure of the *fractional reduction* in the original load carrying area, the eigenvalues of the integrity tensor $\mathbf{\Omega}$ provide a measure of the fraction of the original area that is still available to carry load. Due to the definition of the integrity tensor in Eq. (3), the principal directions of the integrity tensor also coincide with the principal material directions, and the eigenvalues of the integrity tensor Ω_1, Ω_2, and Ω_3 represent the square roots of the available fraction of the original load carrying area on planes that are perpendicular to the 1, 2, and 3 directions respectively.

1.6 *Damaged constitutive relations (stiffness reduction scheme)*

The damage tensor $\mathbf{D}$ and the integrity tensor $\boldsymbol{\Omega}$ can be used to define the concept of *effective* stress $\tilde{\boldsymbol{\sigma}}$. For damaged materials, the definition of the *effective* stress $\tilde{\boldsymbol{\sigma}}$ represents an attempt to assign the actual internal material forces to cross sectional areas that have been reduced due to the presence of damage. Qualitatively speaking, we expect the *effective* stress $\tilde{\boldsymbol{\sigma}}$ to be greater than the apparent stress $\boldsymbol{\sigma}$ (which uses the original undamaged cross sectional area); however, the precise manner of defining the *effective* stress is somewhat arbitrary, and consequently numerous methods have been proposed in the literature (Skrzypek and Ganczarski [10]).

In this study, we use the symmetric effective stress tensor described by Cordebois and Sidornoff [12], which can be expressed as

$$\tilde{\boldsymbol{\sigma}} = \mathbf{M}^{-1}:\boldsymbol{\sigma} = \left(\boldsymbol{\Omega}^{-1}\otimes\boldsymbol{\Omega}^{-1}\right):\boldsymbol{\sigma} = \left(\left(\sqrt{\mathbf{I}-\mathbf{D}}\right)^{-1}\otimes\left(\sqrt{\mathbf{I}-\mathbf{D}}\right)^{-1}\right):\boldsymbol{\sigma}, \tag{4}$$

where $\mathbf{M}$ is the 4th order, doubly symmetric, *damage effect tensor* whose components are $M_{ijkl} = \Omega_{ik}\Omega_{jl}$. Thus as damage accumulates, (i.e. as the D_i increase, or as the Ω_i decrease) the load carrying area decreases which causes the effective stress to increase above the apparent or nominal stress. When the above relationship is expressed in the *principal material coordinate system*, then the 2nd order damage tensor $\mathbf{D}$ and the 2nd order integrity tensor $\boldsymbol{\Omega}$ can be expressed in terms of their eigenvalues:

$$\boldsymbol{\Omega} \rightarrow \begin{bmatrix} \Omega_1 & 0 & 0 \\ 0 & \Omega_2 & 0 \\ 0 & 0 & \Omega_3 \end{bmatrix}, \quad \text{and} \quad \mathbf{D} \rightarrow \begin{bmatrix} D_1 & 0 & 0 \\ 0 & D_2 & 0 \\ 0 & 0 & D_3 \end{bmatrix}.$$

Further, if we represent the effective and apparent stress tensors using *contracted notation*, then we can represent the damage effects tensor $\mathbf{M}$ and its $\mathbf{M}^{-1}$ inverse in the principal material coordinate system as a diagonal 6x6 matrix as follows.

$$\mathbf{M} \rightarrow \begin{bmatrix} \Omega_1^2 & 0 & 0 & 0 & 0 & 0 \\ 0 & \Omega_2^2 & 0 & 0 & 0 & 0 \\ 0 & 0 & \Omega_3^2 & 0 & 0 & 0 \\ 0 & 0 & 0 & \frac{\Omega_2\Omega_3}{2} & 0 & 0 \\ 0 & 0 & 0 & 0 & \frac{\Omega_3\Omega_1}{2} & 0 \\ 0 & 0 & 0 & 0 & 0 & \frac{\Omega_1\Omega_2}{2} \end{bmatrix} \tag{5}$$

$$\mathbf{M}^{-1} \rightarrow \begin{bmatrix} \frac{1}{\Omega_1^2} & 0 & 0 & 0 & 0 & 0 \\ 0 & \frac{1}{\Omega_2^2} & 0 & 0 & 0 & 0 \\ 0 & 0 & \frac{1}{\Omega_3^2} & 0 & 0 & 0 \\ 0 & 0 & 0 & \frac{2}{\Omega_2\Omega_3} & 0 & 0 \\ 0 & 0 & 0 & 0 & \frac{2}{\Omega_3\Omega_1} & 0 \\ 0 & 0 & 0 & 0 & 0 & \frac{2}{\Omega_1\Omega_2} \end{bmatrix} \tag{6}$$

This yields the following expressions for the components of the *effective* stress tensor $\tilde{\boldsymbol{\sigma}}$ expressed in the principal material coordinate system.

$$\tilde{\sigma}_1 = \frac{\sigma_1}{\Omega_1^2} = \frac{\sigma_1}{(1-D_1)}, \tag{7a}$$

$$\tilde{\sigma}_2 = \frac{\sigma_2}{\Omega_2^2} = \frac{\sigma_2}{(1-D_2)}, \tag{7b}$$

$$\tilde{\sigma}_3 = \frac{\sigma_3}{\Omega_3^2} = \frac{\sigma_3}{(1-D_3)}, \tag{7c}$$

$$\tilde{\sigma}_4 = \frac{\sigma_4}{\Omega_2\Omega_3} = \frac{\sigma_4}{\sqrt{1-D_2}\sqrt{1-D_3}}, \tag{7d}$$

$$\tilde{\sigma}_5 = \frac{\sigma_5}{\Omega_3\Omega_1} = \frac{\sigma_5}{\sqrt{1-D_3}\sqrt{1-D_1}}, \tag{7e}$$

$$\tilde{\sigma}_6 = \frac{\sigma_6}{\Omega_1\Omega_2} = \frac{\sigma_6}{\sqrt{1-D_1}\sqrt{1-D_2}}. \tag{7f}$$

We can now define the components of the *effective* strain tensor $\tilde{\boldsymbol{\varepsilon}}$ by insisting that the actual damaged configuration and the fictitious undamaged *effective* configuration should exhibit the same form for the strain energy density. This is the so-called principle of equivalent strain energy, which can be expressed as follows

$$\frac{1}{2}\tilde{\boldsymbol{\sigma}} : \tilde{\boldsymbol{\varepsilon}} = \frac{1}{2}\boldsymbol{\sigma} : \boldsymbol{\varepsilon} \tag{8}$$

Now, substitute the inverse of Eq. (4), i.e., $\boldsymbol{\sigma} = \mathbf{M} : \tilde{\boldsymbol{\sigma}}$.

$$\tilde{\boldsymbol{\sigma}} : \tilde{\boldsymbol{\varepsilon}} = \left(\mathbf{M} : \tilde{\boldsymbol{\sigma}}\right) : \boldsymbol{\varepsilon} \quad \rightarrow \quad \tilde{\boldsymbol{\varepsilon}} : \tilde{\boldsymbol{\sigma}} = \boldsymbol{\varepsilon} : \mathbf{M} : \tilde{\boldsymbol{\sigma}}. \tag{9}$$

Equation (9) must be true for arbitrary $\tilde{\boldsymbol{\sigma}}$, which yields

$$\tilde{\boldsymbol{\varepsilon}} = \boldsymbol{\varepsilon} : \mathbf{M} = \mathbf{M} : \boldsymbol{\varepsilon}. \tag{10a}$$

Thus, based on the principle of equivalent strain energy, the components of the *effective* strain tensor $\tilde{\boldsymbol{\varepsilon}}$ are given by

$$\tilde{\boldsymbol{\varepsilon}} = \mathbf{M} : \boldsymbol{\varepsilon} = (\boldsymbol{\Omega} \otimes \boldsymbol{\Omega}) : \boldsymbol{\varepsilon} = \left(\sqrt{\mathbf{I} - \mathbf{D}}\right) \otimes \left(\sqrt{\mathbf{I} - \mathbf{D}}\right) : \boldsymbol{\varepsilon}, \tag{10b}$$

where $M_{ijkl} = \Omega_{ik}\Omega_{jl}$. When expressed in the principal material coordinate system, the tensors **D**, **Ω**, and **M** can be represented by diagonal matrices, and thus yield the following expressions for the strain components.

$$\tilde{\varepsilon}_1 = \varepsilon_1 \Omega_1^2 = \varepsilon_1 (1 - D_1), \tag{11a}$$

$$\tilde{\varepsilon}_2 = \varepsilon_2 \Omega_2^2 = \varepsilon_2 (1 - D_2), \tag{11b}$$

$$\tilde{\varepsilon}_3 = \varepsilon_3 \Omega_3^2 = \varepsilon_3 (1 - D_3), \tag{11c}$$

$$\tilde{\varepsilon}_4 = \varepsilon_4 \Omega_2 \Omega_3 = \varepsilon_4 \sqrt{1 - D_2}\sqrt{1 - D_3}, \tag{11d}$$

$$\tilde{\varepsilon}_5 = \varepsilon_5 \Omega_3 \Omega_1) = \varepsilon_5 \sqrt{1 - D_3}\sqrt{1 - D_1}, \tag{11e}$$

$$\tilde{\varepsilon}_6 = \varepsilon_6 \Omega_1 \Omega_2) = \varepsilon_6 \sqrt{1 - D_1}\sqrt{1 - D_2}. \tag{11f}$$

The presence of distributed damage, as defined by the internal variable **D,** affects the Helmholtz free energy Ψ, which is postulated to be the sum of elastic strain energy φ and dissipation energy π:

$$\Psi = \Psi(\boldsymbol{\varepsilon}, \mathbf{D}, \delta) = \varphi(\boldsymbol{\varepsilon}, \mathbf{D}) + \pi(\delta). \tag{12}$$

In Eq. (12), we have assumed introduced another internal variable δ, which is a non-dimensional parameter that will be shown later to govern the evolution of the damage tensor **D**.

Assuming that the homogenized composite material exhibits a linear elastic stress/strain relationship up to the point of damage initiation, we can express the strain energy φ in either a strain-based form or stress-based form as follows

$$\varphi(\boldsymbol{\varepsilon}, \mathbf{D}) = \frac{1}{2}\boldsymbol{\varepsilon} : \mathbf{C} : \boldsymbol{\varepsilon} = \frac{1}{2}\boldsymbol{\sigma} : \boldsymbol{\varepsilon}, \tag{13a}$$

$$\varphi(\boldsymbol{\sigma}, \mathbf{D}) = \frac{1}{2}\boldsymbol{\sigma} : \mathbf{C}^{-1} : \boldsymbol{\sigma} = \frac{1}{2}\boldsymbol{\sigma} : \boldsymbol{\varepsilon}, \tag{13b}$$

where $\mathbf{C} = \mathbf{C}(\mathbf{D})$ is the 4th order *damaged* material elasticity tensor, and $\mathbf{C}^{-1} = \mathbf{C}^{-1}(\mathbf{D})$ is the 4th order *damaged* material compliance tensor. The dependence of these two tensors on the damage tensor **D** is defined by requiring that the elastic strain energy of the actual damaged configuration should be equivalent to the stain energy of the fictitious, undamaged *effective* configuration. This strain energy equivalence can be expressed as follows:

$$\varphi(\boldsymbol{\sigma}, \mathbf{D}) = \varphi(\tilde{\boldsymbol{\sigma}}, \mathbf{D}=0) \qquad \text{stress-based} \tag{14a}$$

or

$$\varphi(\boldsymbol{\varepsilon}, \mathbf{D}) = \varphi(\tilde{\boldsymbol{\varepsilon}}, \mathbf{D}=0) \qquad \text{strain-based} \tag{14b}$$

Equations (14a) and (14b) can be written as

$$\frac{1}{2}\boldsymbol{\sigma} : \mathbf{C}^{-1} : \boldsymbol{\sigma} = \frac{1}{2}\tilde{\boldsymbol{\sigma}} : \tilde{\mathbf{C}}^{-1} : \tilde{\boldsymbol{\sigma}}, \tag{15a}$$

$$\frac{1}{2}\boldsymbol{\varepsilon} : \mathbf{C} : \boldsymbol{\varepsilon} = \frac{1}{2}\tilde{\boldsymbol{\varepsilon}} : \tilde{\mathbf{C}} : \tilde{\boldsymbol{\varepsilon}}, \tag{15b}$$

where $\tilde{\mathbf{C}}$ and $\tilde{\mathbf{C}}^{-1}$ represent the stiffness and compliance tensors of the undamaged material.

Substituting Eq. (4) $\tilde{\boldsymbol{\sigma}} = \mathbf{M}^{-1} : \boldsymbol{\sigma}$ into Eq. (15a) and substituting Eq. (10) $\tilde{\boldsymbol{\varepsilon}} = \mathbf{M} : \boldsymbol{\varepsilon}$ into Eq. (15b), and further noting that $\boldsymbol{\sigma} : \mathbf{M}^{-1} = \mathbf{M}^{-1} : \boldsymbol{\sigma}$ and $\boldsymbol{\varepsilon} : \mathbf{M} = \mathbf{M} : \boldsymbol{\varepsilon}$ since $\tilde{\boldsymbol{\sigma}}$ and $\tilde{\boldsymbol{\varepsilon}}$ are both symmetric tensors, we arrive at

$$\frac{1}{2}\boldsymbol{\sigma} : \mathbf{C}^{-1} : \boldsymbol{\sigma} = \frac{1}{2}\boldsymbol{\sigma} : \mathbf{M}^{-1} : \tilde{\mathbf{C}}^{-1} : \mathbf{M}^{-1} : \boldsymbol{\sigma} , \tag{16a}$$

$$\frac{1}{2}\boldsymbol{\varepsilon} : \mathbf{C} : \boldsymbol{\varepsilon} = \frac{1}{2}\boldsymbol{\varepsilon} : \mathbf{M} : \tilde{\mathbf{C}} : \mathbf{M} : \boldsymbol{\varepsilon} . \tag{16b}$$

Equations (16a,b) must be valid for any arbitrary $\boldsymbol{\sigma}$ and $\boldsymbol{\varepsilon}$. Therefore, Eq. (16a) yields the following expressions for the *damaged* compliance tensor

$$\mathbf{C}^{-1} = \mathbf{M}^{-1} : \tilde{\mathbf{C}}^{-1} : \mathbf{M}^{-1} , \tag{17a}$$

$$\mathbf{C}^{-1} = \left(\boldsymbol{\Omega}^{-1} \otimes \boldsymbol{\Omega}^{-1}\right) : \tilde{\mathbf{C}}^{-1} : \left(\boldsymbol{\Omega}^{-1} \otimes \boldsymbol{\Omega}^{-1}\right) , \tag{17b}$$

$$\mathbf{C}^{-1} = \left(\left(\sqrt{\mathbf{I} - \mathbf{D}}\right)^{-1} \otimes \left(\sqrt{\mathbf{I} - \mathbf{D}}\right)^{-1}\right) : \tilde{\mathbf{C}}^{-1} : \left(\left(\sqrt{\mathbf{I} - \mathbf{D}}\right)^{-1} \otimes \left(\sqrt{\mathbf{I} - \mathbf{D}}\right)^{-1}\right) , \tag{17c}$$

and Eq. (16b) yields the following expressions for the *damaged* stiffness tensor.

$$\mathbf{C} = \mathbf{M} : \tilde{\mathbf{C}} : \mathbf{M} , \tag{18a}$$

$$\mathbf{C} = (\boldsymbol{\Omega} \otimes \boldsymbol{\Omega}) : \tilde{\mathbf{C}} : (\boldsymbol{\Omega} \otimes \boldsymbol{\Omega}) , \tag{18b}$$

$$\mathbf{C} = \left(\left(\sqrt{\mathbf{I} - \mathbf{D}}\right) \otimes \left(\sqrt{\mathbf{I} - \mathbf{D}}\right)\right) : \tilde{\mathbf{C}} : \left(\left(\sqrt{\mathbf{I} - \mathbf{D}}\right) \otimes \left(\sqrt{\mathbf{I} - \mathbf{D}}\right)\right) . \tag{18c}$$

Eqs. (17) and (18) define the *damaged* 4th order compliance tensor $\mathbf{C}^{-1}$ and the *damaged* 4th order elasticity tensor $\mathbf{C}$ in terms of the 4th order damage effects tensor $\mathbf{M}$, the 2nd order integrity tensor $\boldsymbol{\Omega}$ and the 2nd order damage tensor $\mathbf{D}$.

Expressing Eqs. (18a-c) in the principal material coordinate system and using contracted notation, the resulting 4th order, *damaged* material elasticity tensor $\mathbf{C}$ can be represented by the following 6x6 matrix which is indicative of an *orthotropically damaged* material.

$$\mathbf{C} \rightarrow \begin{bmatrix} C_{11} & C_{12} & C_{13} & 0 & 0 & 0 \\ C_{21} & C_{22} & C_{23} & 0 & 0 & 0 \\ C_{31} & C_{32} & C_{33} & 0 & 0 & 0 \\ 0 & 0 & 0 & C_{44} & 0 & 0 \\ 0 & 0 & 0 & 0 & C_{55} & 0 \\ 0 & 0 & 0 & 0 & 0 & C_{66} \end{bmatrix} . \tag{19}$$

The individual components of the damaged orthotropic material elasticity tensor are defined as

$$C_{11} = \tilde{C}_{11}\Omega_1^4 = \tilde{C}_{11}(1-D_1)^2 , \tag{20a}$$

$$C_{12} = \tilde{C}_{12}\Omega_1^2\Omega_2^2 = \tilde{C}_{12}(1-D_1)(1-D_2) = C_{21} , \tag{20b}$$

$$C_{13} = \tilde{C}_{13}\Omega_1^2\Omega_3^2 = \tilde{C}_{13}(1-D_1)(1-D_3) = C_{31} , \tag{20c}$$

$$C_{22} = \tilde{C}_{22}\Omega_2^4 = \tilde{C}_{22}(1-D_2)^2 , \tag{20d}$$

$$C_{23} = \tilde{C}_{23}\Omega_2^2\Omega_3^2 = \tilde{C}_{23}(1-D_2)(1-D_3) = C_{32} , \tag{20e}$$

$$C_{33} = \tilde{C}_{33}\Omega_3^4 = \tilde{C}_{33}(1-D_3)^2 , \tag{20f}$$

$$C_{44} = \frac{1}{2}\tilde{C}_{44}\Omega_2^2\Omega_3^2 = \frac{1}{2}\tilde{C}_{44}(1-D_2)(1-D_3) , \tag{20g}$$

$$C_{55} = \frac{1}{2}\tilde{C}_{55}\Omega_3^2\Omega_1^2 = \frac{1}{2}\tilde{C}_{55}(1-D_3)(1-D_1) , \tag{20h}$$

$$C_{66} = \frac{1}{2}\tilde{C}_{66}\Omega_1^2\Omega_2^2 = \frac{1}{2}\tilde{C}_{66}(1-D_1)(1-D_2) . \tag{20i}$$

Similarly, the individual components of the damaged orthotropic material compliance tensor are expressed in the principal material coordinate system as

$$C_{11}^{-1} = \frac{\tilde{C}_{11}^{-1}}{\Omega_1^4} = \frac{\tilde{C}_{11}^{-1}}{(1-D_1)^2} , \tag{21a}$$

$$C_{12}^{-1} = \frac{\tilde{C}_{12}^{-1}}{\Omega_1^2\,\Omega_2^2} = \frac{\tilde{C}_{12}^{-1}}{(1-D_1)(1-D_2)} = C_{21}^{-1} , \tag{21b}$$

$$C_{13}^{-1} = \frac{\tilde{C}_{13}^{-1}}{\Omega_1^2\,\Omega_3^2} = \frac{\tilde{C}_{13}^{-1}}{(1-D_1)(1-D_3)} = C_{31}^{-1} , \tag{21c}$$

$$C_{22}^{-1} = \frac{\tilde{C}_{22}^{-1}}{\Omega_2^4} = \frac{\tilde{C}_{22}^{-1}}{(1-D_2)^2} , \tag{21d}$$

$$C_{23}^{-1} = \frac{\tilde{C}_{23}^{-1}}{\Omega_2^2\,\Omega_3^2} = \frac{\tilde{C}_{23}^{-1}}{(1-D_2)(1-D_3)} = C_{32}^{-1} , \tag{21e}$$

$$C_{33}^{-1} = \frac{\tilde{C}_{33}^{-1}}{\Omega_3^4} = \frac{\tilde{C}_{33}^{-1}}{(1-D_3)^2} \tag{21f}$$

$$C_{44}^{-1} = \frac{2\tilde{C}_{44}^{-1}}{\Omega_2^2\,\Omega_3^2} = \frac{2\tilde{C}_{44}^{-1}}{(1-D_2)(1-D_3)} , \tag{21g}$$

$$C_{55}^{-1} = \frac{2\tilde{C}_{55}^{-1}}{\Omega_3^2\,\Omega_1^2} = \frac{2\tilde{C}_{55}^{-1}}{(1-D_3)(1-D_1)} , \tag{21h}$$

$$C_{66}^{-1} = \frac{2\tilde{C}_{66}^{-1}}{\Omega_1^2\,\Omega_2^2} = \frac{2\tilde{C}_{66}^{-1}}{(1-D_1)(1-D_2)} . \tag{21i}$$

1.7 *Damaged surface*

For the independent kinematic state variables ($\boldsymbol{\varepsilon}$, $\mathbf{D}$, δ) that are used to express the Helmholtz free energy, the associated energy conjugate variables (i.e. thermodynamic forces) are obtained by partial differentiation of Ψ with respect to the kinematic variables.

Partial differentiation of $\rho\Psi$ with respect to the strain tensor $\boldsymbol{\varepsilon}$ yields the stress tensor $\boldsymbol{\sigma}$ that acts on the damaged configuration.

$$\boldsymbol{\sigma} = \rho\partial\Psi/\partial\boldsymbol{\varepsilon} = \mathbf{C} : \boldsymbol{\varepsilon} = \left(\mathbf{M}:\tilde{\mathbf{C}}:\mathbf{M}\right) : \boldsymbol{\varepsilon} . \tag{22}$$

Partial differentiation of Ψ with respect to the damage tensor **D** yields the energy release rate tensor **Y**, so named because it represents the energy released per unit increase of the damage tensor.

$$\mathbf{Y} = -\rho\frac{\partial\Psi(\boldsymbol{\varepsilon},\mathbf{D},\delta)}{\partial\mathbf{D}} = -\rho\frac{\partial\varphi(\boldsymbol{\varepsilon},\mathbf{D})}{\partial\mathbf{D}} = -\frac{\partial\left(\frac{1}{2}\boldsymbol{\varepsilon}:\mathbf{C}:\boldsymbol{\varepsilon}\right)}{\partial\mathbf{D}}. \tag{23}$$

In Eq. (24), $\mathbf{C} = \mathbf{C}(\mathbf{D})$, while $\boldsymbol{\varepsilon}$ is independent of **D**.

$$\mathbf{Y} = -\frac{\partial\left(\frac{1}{2}\boldsymbol{\varepsilon}:\mathbf{C}:\boldsymbol{\varepsilon}\right)}{\partial\mathbf{D}} = -\frac{1}{2}\boldsymbol{\varepsilon}:\frac{\partial\mathbf{C}}{\partial\mathbf{D}}:\boldsymbol{\varepsilon} = -\frac{1}{2}\boldsymbol{\varepsilon}:\frac{\partial\left(\mathbf{M}:\tilde{\mathbf{C}}:\mathbf{M}\right)}{\partial\mathbf{D}}:\boldsymbol{\varepsilon}, \tag{24a}$$

$$\mathbf{Y} = -\frac{1}{2}\boldsymbol{\varepsilon}:\frac{\partial\mathbf{M}}{\partial\mathbf{D}}:\tilde{\mathbf{C}}:\mathbf{M}:\boldsymbol{\varepsilon} - \frac{1}{2}\boldsymbol{\varepsilon}:\mathbf{M}:\tilde{\mathbf{C}}:\frac{\partial\mathbf{M}}{\partial\mathbf{D}}:\boldsymbol{\varepsilon} = -\boldsymbol{\varepsilon}:\frac{\partial\mathbf{M}}{\partial\mathbf{D}}:\tilde{\mathbf{C}}:\mathbf{M}:\boldsymbol{\varepsilon}. \tag{24b}$$

When Eq. (24) is evaluated in the principal material coordinate system, the energy release rate tensor **Y** is diagonal and its eigenvalues Y_i (i=1,2,3) are expressed in terms of the actual strains, the undamaged stiffness and the eignevalues of the integrity tensor as

$$Y_1 = \tilde{C}_{11}\Omega_1^2\varepsilon_1^2 + \tilde{C}_{12}\Omega_2^2\varepsilon_1\varepsilon_2 + \tilde{C}_{13}\Omega_3^2\varepsilon_1\varepsilon_3 + \tilde{C}_{55}\Omega_3^2\varepsilon_5^2 + \tilde{C}_{66}\Omega_2^2\varepsilon_6^2, \tag{25a}$$

$$Y_2 = \tilde{C}_{21}\Omega_1^2\varepsilon_1\varepsilon_2 + \tilde{C}_{22}\Omega_2^2\varepsilon_2^2 + \tilde{C}_{23}\Omega_3^2\varepsilon_2\varepsilon_3 + \tilde{C}_{44}\Omega_3^2\varepsilon_5^2 + \tilde{C}_{66}\Omega_1^2\varepsilon_6^2, \tag{25b}$$

$$Y_3 = \tilde{C}_{11}\Omega_1^2\varepsilon_1\varepsilon_3 + \tilde{C}_{32}\Omega_2^2\varepsilon_2\varepsilon_3 + \tilde{C}_{23}\Omega_3^2\varepsilon_3^2 + \tilde{C}_{44}\Omega_2^2\varepsilon_5^2 + \tilde{C}_{55}\Omega_1^2\varepsilon_5^2. \tag{25c}$$

Substituting Eqs. (20a-i) into Eqs. (25a-c), the eigenvalues of the energy release rate tensor Y_i (i=1,2,3) can be expressed in terms of the actual damaged stiffness tensor, the actual strain tensor and the integrity tensor:

$$Y_1 = \frac{1}{\Omega_1^2}\left(C_{11}\varepsilon_1^2 + C_{12}\varepsilon_1\varepsilon_2 + C_{13}\varepsilon_1\varepsilon_3 + C_{55}\varepsilon_5^2 + C_{66}\varepsilon_6^2\right), \tag{26a}$$

$$Y_2 = \frac{1}{\Omega_2^2}\left(C_{21}\varepsilon_1\varepsilon_2 + C_{22}\varepsilon_2^2 + C_{23}\varepsilon_2\varepsilon_3 + C_{44}\varepsilon_5^2 + C_{66}\varepsilon_6^2\right), \tag{26b}$$

$$Y_3 = \frac{1}{\Omega_3^2}\left(C_{11}\varepsilon_1\varepsilon_3 + C_{32}\varepsilon_2\varepsilon_3 + C_{23}\varepsilon_3^2 + C_{44}\varepsilon_5^2 + C_{55}\varepsilon_5^2\right). \tag{26c}$$

Note that the potential φ in Eq. (23) can alternately be expressed using $\tilde{\boldsymbol{\varepsilon}}(\mathbf{D})$ and $\tilde{\mathbf{C}}$, instead of $\boldsymbol{\varepsilon}$ and **C**, which would yield

$$\mathbf{Y} = -\rho\partial\Psi/\partial\mathbf{D} = -\rho\partial\varphi/\partial\mathbf{D} = -\frac{\partial\left(\frac{1}{2}\tilde{\boldsymbol{\varepsilon}}:\tilde{\mathbf{C}}:\tilde{\boldsymbol{\varepsilon}}\right)}{\partial\mathbf{D}}, \tag{27a}$$

$$\mathbf{Y} = -\frac{\partial\left(\frac{1}{2}\tilde{\boldsymbol{\varepsilon}}:\tilde{\mathbf{C}}:\tilde{\boldsymbol{\varepsilon}}\right)}{\partial\mathbf{D}} = -\frac{1}{2}\frac{\partial\tilde{\boldsymbol{\varepsilon}}}{\partial\mathbf{D}}:\tilde{\mathbf{C}}:\tilde{\boldsymbol{\varepsilon}} - \frac{1}{2}\tilde{\boldsymbol{\varepsilon}}:\tilde{\mathbf{C}}:\frac{\partial\tilde{\boldsymbol{\varepsilon}}}{\partial\mathbf{D}} = -\frac{\partial\tilde{\boldsymbol{\varepsilon}}}{\partial\mathbf{D}}:\tilde{\mathbf{C}}:\tilde{\boldsymbol{\varepsilon}}. \tag{27b}$$

When evaluated in the principal material coordinate system, Eq. (27b) yields the same expressions for the eigenvalues of **Y** as obtained earlier in Eqs. (25) and (26).

We can express the energy release rate tensor **Y** in terms of stress components by utilizing the dual of the potential φ as follows

$$\boldsymbol{\sigma} : \boldsymbol{\varepsilon} \;=\; \varphi(\boldsymbol{\varepsilon},\mathbf{D}) \;+\; \varphi^*(\boldsymbol{\sigma},\mathbf{D}) \qquad \rightarrow \qquad \varphi(\boldsymbol{\varepsilon},\mathbf{D}) \;=\; \boldsymbol{\sigma} : \boldsymbol{\varepsilon} \;-\; \varphi^*(\boldsymbol{\sigma},\mathbf{D})\,. \tag{28}$$

Thus the energy release rate tensor can be expressed in either of the following ways.

$$\mathbf{Y} \;=\; -\,\rho\,\frac{\partial \varphi}{\partial \mathbf{D}} \;=\; \rho\,\frac{\partial \varphi^*}{\partial \mathbf{D}}\,, \tag{29}$$

$$\text{where} \quad \varphi^*(\boldsymbol{\sigma},\mathbf{D}) \;=\; \frac{1}{2}\,\boldsymbol{\sigma} : \mathbf{C}^{-1} : \boldsymbol{\sigma} \quad \text{and} \quad \mathbf{C}^{-1} = \mathbf{C}^{-1}(\mathbf{D}). \tag{30}$$

Substituting Eq. (30) into Eq. (29) yields

$$\mathbf{Y} \;=\; \frac{\partial\left(\frac{1}{2}\,\boldsymbol{\sigma} : \mathbf{C}^{-1} : \boldsymbol{\sigma}\right)}{\partial \mathbf{D}} \;=\; \frac{1}{2}\,\boldsymbol{\sigma} : \frac{\partial \mathbf{C}^{-1}}{\partial \mathbf{D}} : \boldsymbol{\sigma} \;=\; \frac{1}{2}\,\boldsymbol{\sigma} : \frac{\partial\left(\mathbf{M}^{-1} : \tilde{\mathbf{C}}^{-1} : \mathbf{M}^{-1}\right)}{\partial \mathbf{D}} : \boldsymbol{\sigma}\,, \tag{31a}$$

$$\mathbf{Y} \;=\; -\frac{1}{2}\,\boldsymbol{\sigma} : \frac{\partial \mathbf{M}^{-1}}{\partial \mathbf{D}} : \tilde{\mathbf{C}}^{-1} : \mathbf{M}^{-1} : \boldsymbol{\sigma} \;-\; \frac{1}{2}\,\boldsymbol{\sigma} : \mathbf{M}^{-1} : \tilde{\mathbf{C}}^{-1} : \frac{\partial \mathbf{M}^{-1}}{\partial \mathbf{D}} : \boldsymbol{\sigma} \;=\; -\,\boldsymbol{\sigma} : \frac{\partial \mathbf{M}^{-1}}{\partial \mathbf{D}} : \tilde{\mathbf{C}}^{-1} : \mathbf{M}^{-1} : \boldsymbol{\sigma}\,. \tag{31b}$$

When Eq. (31b) is evaluated in the principal material coordinate system, the eigenvalues of the energy release rate tensor Y_i (i=1,2,3) can be expressed in terms of the undamaged compliance tensor, the actual stress tensor, and the integrity tensor as follows.

$$Y_1 \;=\; \frac{2}{\Omega_1^4}\left(\frac{\tilde{C}_{11}^{-1}}{\Omega_1^2}\sigma_1^2 \;+\; \frac{\tilde{C}_{12}^{-1}}{\Omega_2^2}\,\sigma_1\sigma_2 \;+\; \frac{\tilde{C}_{13}^{-1}}{\Omega_3^2}\,\sigma_1\sigma_3 \;+\; \frac{\tilde{C}_{55}^{-1}}{\Omega_3^2}\,\sigma_5^2 \;+\; \frac{\tilde{C}_{66}^{-1}}{\Omega_2^2}\,\sigma_6^2\right), \tag{32a}$$

$$Y_2 \;=\; \frac{2}{\Omega_2^4}\left(\frac{\tilde{C}_{21}^{-1}}{\Omega_1^2}\,\sigma_1\sigma_2 \;+\; \frac{\tilde{C}_{22}^{-1}}{\Omega_2^2}\,\sigma_2^2 \;+\; \frac{\tilde{C}_{23}^{-1}}{\Omega_3^2}\,\sigma_2\sigma_3 \;+\; \frac{\tilde{C}_{44}^{-1}}{\Omega_3^2}\,\sigma_4^2 \;+\; \frac{\tilde{C}_{66}^{-1}}{\Omega_1^2}\,\sigma_6^2\right), \tag{32b}$$

$$Y_3 \;=\; \frac{2}{\Omega_3^4}\left(\frac{\tilde{C}_{31}^{-1}}{\Omega_1^2}\,\sigma_1\sigma_3 \;+\; \frac{\tilde{C}_{32}^{-1}}{\Omega_2^2}\,\sigma_2\sigma_3 \;+\; \frac{\tilde{C}_{33}^{-1}}{\Omega_3^2}\,\sigma_3^2 \;+\; \frac{\tilde{C}_{44}^{-1}}{\Omega_2^2}\,\sigma_4^2 \;+\; \frac{\tilde{C}_{55}^{-1}}{\Omega_1^2}\,\sigma_5^2\right). \tag{32c}$$

Substituting Eqs. (21) into Eqs. (31), the eigenvalues of the energy release rate tensor can be expressed in terms of the actual damaged compliance tensor, the actual stress tensor and the integrity tensor.

$$Y_1 \;=\; \frac{2}{\Omega_1^2}\left(C_{11}^{-1}\,\sigma_1^2 \;+\; C_{12}^{-1}\,\sigma_1\sigma_2 \;+\; C_{13}^{-1}\,\sigma_1\sigma_3 \;+\; C_{55}^{-1}\,\sigma_5^2 \;+\; C_{66}^{-1}\,\sigma_6^2\right), \tag{33a}$$

$$Y_2 \;=\; \frac{2}{\Omega_2^2}\left(C_{21}^{-1}\,\sigma_2\sigma_1 \;+\; C_{22}^{-1}\,\sigma_2^2 \;+\; C_{23}^{-1}\,\sigma_2\sigma_3 \;+\; C_{44}^{-1}\,\sigma_4^2 \;+\; C_{66}^{-1}\,\sigma_6^2\right), \tag{33b}$$

$$Y_3 \;=\; \frac{2}{\Omega_3^3}\left(C_{31}^{-1}\,\sigma_3\sigma_1 \;+\; C_{32}^{-1}\,\sigma_3\sigma_2 \;+\; C_{33}^{-1}\,\sigma_3^2 \;+\; C_{44}^{-1}\,\sigma_4^2 \;+\; C_{55}^{-1}\,\sigma_5^2\right). \tag{33c}$$

Equation. (32) and (33) can also be obtained by expressing the dual potential φ^* in terms of the effective stress $\tilde{\boldsymbol{\sigma}}$ and the undamaged compliance $\tilde{\mathbf{C}}^{-1}$, i.e., $\varphi^*(\boldsymbol{\sigma},\mathbf{D}) \;=\; \frac{1}{2}\,\tilde{\boldsymbol{\sigma}} : \tilde{\mathbf{C}}^{-1} : \tilde{\boldsymbol{\sigma}}$ where $\tilde{\boldsymbol{\sigma}} = \tilde{\boldsymbol{\sigma}}(\mathbf{D})$ and $\tilde{\mathbf{C}}^{-1}$ is independent of $\mathbf{D}$.

The damage surface, which is assumed to separate non-damaging behavior from damage-inducing behavior, is defined as a complete quadratic function of the energy release rate tensor.

$$g(\mathbf{Y},\gamma) = \sqrt{\mathbf{Y:J:Y}} + \sqrt{|\mathbf{H:Y}|} - (\gamma(\delta) + \gamma_0). \tag{34}$$

In Eqs. (33), the 4th order tensor **J** and the 2nd order tensor **H** represent experimentally derived material constants that define the damage tolerance of the material. When expressed in the principal material coordinate system, **J** and **H** are each assumed to have only three non-zero values, denoted $J_{11} \equiv J_{1111}$, $J_{22} \equiv J_{2222}$, $J_{33} \equiv J_{3333}$, $H_1 \equiv H_{11}$, $H_2 \equiv H_{22}$, $H_3 \equiv H_{33}$. These six material constants define the *shape* of the damage surface. The material parameter γ_0 is also determined from experimental data and defines the initial *size* of the damage surface, thus functioning as an initial damage threshold. In Eq. (33), the linear term **H:Y** is necessary to define a material that has different damage tolerance in tension and compression. When expressed in the principal material coordinate system, the damage surface simplifies to the following form.

$$g(\mathbf{Y},\gamma) = \sqrt{J_{11}Y_1^2 + J_{22}Y_2^2 + J_{33}Y_3^2} + \sqrt{|H_1Y_1 + H_2Y_2 + H_3Y_3|} - (\gamma(\delta) + \gamma_0) \tag{35}$$

Depending upon whether the energy release rate eigenvalues Y_i (i=1,2,3) are expressed using Eqs. (25), (26), (32), or (33), the damage surface can be defined in terms of either of the following sets of variables: $(\mathbf{C},\boldsymbol{\Omega},\boldsymbol{\varepsilon},\gamma)$, $(\tilde{\mathbf{C}},\boldsymbol{\Omega},\boldsymbol{\varepsilon},\gamma)$, $(\mathbf{C}^{-1},\boldsymbol{\Omega},\boldsymbol{\sigma},\gamma)$, or $(\tilde{\mathbf{C}}^{-1},\boldsymbol{\Omega},\boldsymbol{\sigma},\gamma)$.

The damage surface defined by Eq. (35) has the shape of the Tsai-Wu failure surface when it is expressed in stress space. This can be seen by noting that the energy release rate eigenvalues [Eqs. (32) or (33)] are quadratic functions of the stress components, thus the damage surface [Eq. (35)] can be expressed as

$$g(\mathbf{Y},\gamma) = \beta_{ij}\sigma_i\sigma_j + \alpha_i\sigma_i - (\gamma + \gamma_0) \qquad i,j = 1,2,\ldots,6 \ , \tag{36a}$$

where the coefficients β_{ij}, and α_i are functions of the damaged compliance tensor $\mathbf{C}^{-1}(\mathbf{D})$, the integrity tensor $\boldsymbol{\Omega}(\mathbf{D})$, and the material damage characteristic tensors **J** and **H**. The Tsai-Wu failure criterion [13] predicts failure when

$$F_{ij}\sigma_i\sigma_j + F_i\sigma_i \geq 1 \qquad i,j = 1,2,\ldots,6 \ , \tag{36b}$$

where the coefficients F_{ij} and F_i are functions of the lamina strength in the various modes of deformation.

If we choose to define the quantities γ and γ_0 such that the expression $(\gamma + \gamma_0) = 1$ indicates complete failure of a lamina, then the damage surface $g(\mathbf{Y},\gamma)$ increases failure in the same manner as the Tsai-Wu criterion [13].

The damage surface [Eq. (35)] defines the limits of non-damaging behavior at an arbitrary point in the lamina. If the current local values of Y_i (i=1,2,3) and γ yield a point on the surface $g(\mathbf{Y},\gamma)$, then further damage is assumed to occur. The damage-flow surface, denoted as $f(\mathbf{Y},\gamma)$, is defined similar to the damage surface $g(\mathbf{Y},\gamma)$ but without the linear term **H:Y**.

$$f(\mathbf{Y},\gamma) = \sqrt{\mathbf{Y:J:Y}} - (\gamma(\delta) + \gamma_0) = \sqrt{J_{11}Y_1^2 + J_{22}Y_2^2 + J_{33}Y_3^2} - (\gamma(\delta) + \gamma_0). \tag{36c}$$

1.8 *Damage evolution*

The dissipation potential π is assumed to be of the form

$$\pi(\delta) = -c_1\left(\delta + c_2 \exp\left(\frac{\delta}{c_2}\right)\right) \quad , \tag{37}$$

where the dimensionless parameter $\delta>0$ controls the evolution of the damage process. This is the simplest dissipation potential with the minimum number of adjustable coefficients that still captures the experimentally observed behavior of fiber-reinforced composite laminae. The evolution law is assumed to be isotropic for simplicity and due to the lack of experimental observations indicating anisotropic evolution of the damage surface (Barbero and DeVivo [11]).

The energy conjugate variable to δ is denoted as γ and is obtained by partial differentiation of the free energy with respect to δ:

$$\gamma = -\frac{\partial \psi}{\partial \delta} = -\frac{\partial \pi}{\partial \delta} = c_1\left(1 + \exp\left(\frac{\delta}{c_2}\right)\right). \tag{38a}$$

The evolution of the damage tensor $\mathbf{D}$ occurs in a direction that is normal to the damage-flow surface as defined by Eq. (36c):

$$\dot{\mathbf{D}} = \mu \frac{\partial f(\mathbf{Y},\gamma)}{\partial \mathbf{Y}} = \mu \frac{\mathbf{J:Y}}{\sqrt{\mathbf{Y:J:Y}}} = \mu \frac{J_{11}Y_1 + J_{22}Y_2 + J_{33}Y_3}{\sqrt{J_{11}Y_1^2 + J_{22}Y_2^2 + J_{33}Y_3^2}}. \tag{38b}$$

The evolution of the damage surface is given by

$$\dot{\delta} = \mu \frac{\partial g(\mathbf{Y},\gamma)}{\partial \gamma} = \mu(-1) = -\mu. \tag{38c}$$

In the interest of keeping the size of the report in reasonable limit, numerical results based on the damage models discussed herein are not reported. They will appear in the literature in the near future.

2. Finite Element Formulation of the Layerwise Theory

2.1 *Introductory comments*

The layerwise theory proposed by Reddy [14-16] exploits the laminate architecture to separate the thickness variation from the surface variations and the thickness variation is represented independently using Lagrange polynomials. Reddy and Mitchell [17] presented a general formulation of the problem using both ESL and layerwise theories. Layerwise finite element models of Reddy's layerwise theory can be found in [14-16]. The work of Saravanos et al. [18] is perhaps the first one to use a layerwise finite element model for the analysis of piezoelectric plates. However, these authors only considered constant and linear approximation schemes across the thickness.

In the present study, a general, displacement finite element formulation of the layerwise theory of Reddy [14-16] for laminated plate structures with piezoelectric materials (layers or patches) is developed. The formulation includes full electromechanical coupling and arbitrary approximation through the thickness as well as in the surface of the laminate. Several approximations are used for the primary variables of the problem in the thickness direction and different interpolation schemes are considered in the surface directions.

2.2 *Theoretical formulation*

Consider a laminated plate with thickness H and arbitrary planar geometry, built with piezoelectric laminae or patches and laminae made with different linear elastic materials. A global orthonormal rectangular reference frame (x,y,z) with the z axis aligned with the laminate thickness is assumed. The material within each layer of the laminate is assumed to be homogeneous, generally anisotropic and linear elastic, including linear piezoelectric effects. The constitutive law considered for a composite material is [19-21]:

$$S_{ij} = C^{(k)}_{ijlm} e_{lm} \; ; \quad D_i = X^{(k)}_{il} E_l \tag{39}$$

and for a piezoelectric material:

$$S_{ij} = C^{(k)}_{ijlm} e_{lm} - e^{(k)}_{lij} E_l \; ; \quad D_i = X^{(k)}_{il} E_l + e^{(k)}_{ilm} e_{lm} \tag{40}$$

where S_{ij} and e_{lm} are the components of the stress and strain tensors, D_i and E_i are the electric displacement and electric field vector components, C_{ijlm} are the components of the fourth-order tensor of elastic moduli, e_{lij} are the components of piezoelectric moduli and x_{il} are the components of the dielectric moduli for the k^{th} lamina. The constitutive behaviour of piezoelectric materials makes a piezolaminated structure a coupled mechanical and electrical problem.

The equilibrium of stresses at the interface between adjacent plies (k) and $(k+1)$ requires the stress field to satisfy the conditions (see Figure 1)

$$\begin{Bmatrix} S_{xz} \\ S_{yz} \\ S_{zz} \end{Bmatrix}^{(k)} = \begin{Bmatrix} S_{xz} \\ S_{yz} \\ S_{zz} \end{Bmatrix}^{(k+1)} \tag{41}$$

The electric displacements at the interface must satisfy:

$$D_z^{(k+1)} - D_z^{(k)} = w_e \tag{42}$$

where w_e is the imposed surface charge. If no electric potential is prescribed along the interface, or equivalently no surface charge is imposed, the electric displacement D_z component will be continuous across the interface. Because, in general, the material properties differ for layers (k) and $(k+1)$, conditions (41) and (42) can only be satisfied if:

$$\begin{Bmatrix} e_{xz} \\ e_{yz} \\ e_{zz} \end{Bmatrix}^{(k)} \neq \begin{Bmatrix} e_{xz} \\ e_{yz} \\ e_{zz} \end{Bmatrix}^{(k+1)} , \qquad E_z^{(k)} \neq E_z^{(k+1)} . \tag{43}$$

These conditions imply that the displacement and electric fields must be C^0 continuous in the thickness direction, along the interfaces joining dissimilar materials. Hence, the primary variables, namely, the displacement field components (u, v, w) and electric potential φ, are represented as products of functions of (x,y,t) and C^0 continuous functions of the thickness coordinate z (the upper indices are not exponents):

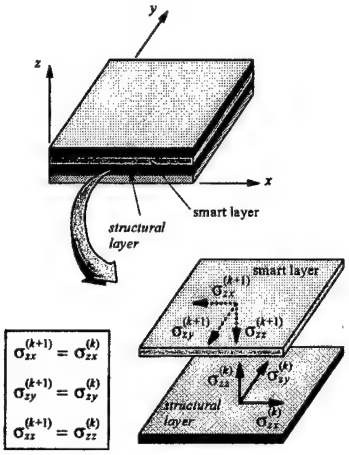

Figure 1: Equilibrium of interlaminar stresses.

$$u(x,y,z,t) = \sum_{I=1}^{N_F} U^I(x,y,t)F^I(z);\quad v(x,y,z,t) = \sum_{I=1}^{N_F} V^I(x,y,t)F^I(z)$$
$$w(x,y,z,t) = \sum_{I=1}^{N_Y} W^I(x,y,t)Y^I(z);\quad j(x,y,z,t) = \sum_{I=1}^{N_Q} J^I(x,y,t)Q^I(z) \tag{44}$$

Following the approach proposed by Reddy [14], the thickness direction C^0 continuous functions $F^I(z)$, $Y^I(z)$ and $Q^I(z)$ are constructed using the Lagrange polynomials and have the following characteristics:

(a) $$F^I(z_J) = d_{IJ};\quad Y^I(z_J) = d_{IJ};\quad Q^I(z_J) = d_{IJ};\quad \text{where}\quad d_{IJ} = \begin{cases} 1, & I = J \\ 0, & I \neq J \end{cases} \tag{45}$$

(b) local support, the functions are nonzero only in the layers that share the Ith interface (see Figure 2).

With this approach several finite element models can be constructed in an efficient and straightforward manner.

The unknowns for the this layerwise theory are the surface functions $U^I(x,y,t)$, $V^I(x,y,t)$, $W^I(x,y,t)$ and $j^I(x,y,t)$. The number of functions N_F , N_Y and N_Q , considered by the theory, depend on the number of layers and on the degree of the assumed approximation along the thickness of each layer for each one of the primary variables. Underlying this assumption for the primary variables is the hypothesis that the behaviour of these fields along the surface directions (x,y), is different from the behavior along the thickness direction (z). This is an assumption common to all the plate and shell theories, that allows reducing a three-dimensional problem to a two-dimensional one.

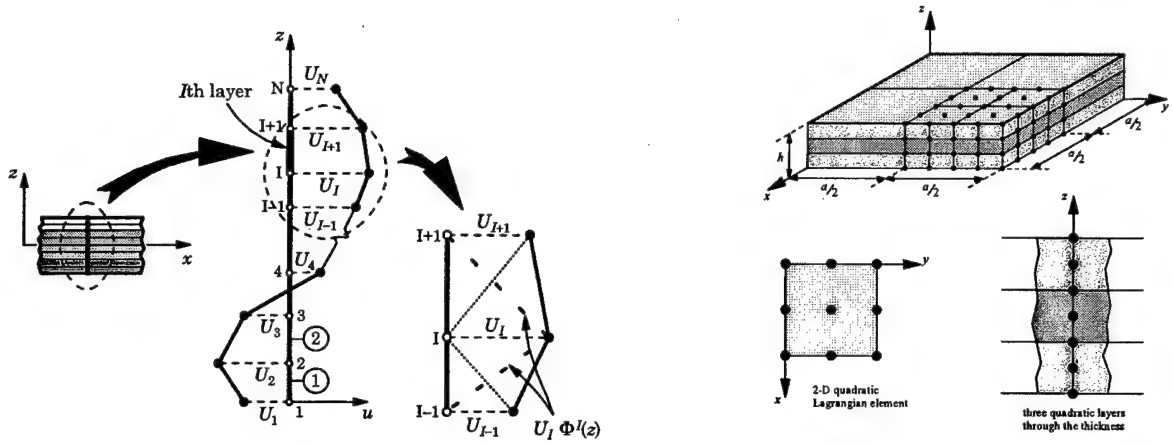

Figure 2. (a) Layer-wise displacement field. (b) Laywerwise representation of a laminate.

The layerwise finite element models are developed using a variational formulation. For details on the theory and variational formulation of the layerwise theory, the reader may consult References 14 through 16. To obtain the finite element model, the primary variables are approximated inside each element as:

$$u(x,y,z,t)=\sum_{I=1}^{N_E}\left(\sum_{K=1}^{N_U^I}U_K^I(t)\,a_K^I(x,y)\right)F^I(z);\quad v(x,y,z,t)=\sum_{I=1}^{N_E}\left(\sum_{K=1}^{N_V^I}V_K^I(t)\,b_K^I(x,y)\right)F^I(z)$$
$$w(x,y,z,t)=\sum_{I=1}^{N_Y}\left(\sum_{K=1}^{N_W^I}W_K^I(t)\,c_K^I(x,y)\right)Y^I(z);\quad j(x,y,z,t)=\sum_{I=1}^{N_Q}\left(\sum_{K=1}^{N_J^I}J_K^I(t)\,f_K^I(x,y)\right)Q^I(z) \tag{46}$$

The numbers N_U^I, N_V^I, N_W^I and N_J^I of interpolation functions $a_K^I(x,y,t)$, $b_K^I(x,y,t)$, $c_K^I(x,y,t)$ and $f_K^I(x,y,t)$, depend of the interpolation scheme associated with the Ith layer thickness function inside the element.This set of equations can be cast in a matrix form:

$$\begin{bmatrix}[M_{uu}] & [0] & [0] & [0]\\ [0] & [M_{vv}] & [0] & [0]\\ [0] & [0] & [M_{ww}] & [0]\\ [0] & [0] & [0] & [0]\end{bmatrix}\begin{Bmatrix}\{\ddot{U}\}\\ \{\ddot{V}\}\\ \{\ddot{W}\}\\ \{\ddot{J}\}\end{Bmatrix}+\begin{bmatrix}[K_{uu}] & [K_{uv}] & [K_{uw}] & [K_{uj}]\\ [K_{vu}] & [K_{vv}] & [K_{vw}] & [K_{vj}]\\ [K_{wu}] & [K_{wv}] & [K_{ww}] & [K_{wj}]\\ [K_{ju}] & [K_{jv}] & [K_{jj}] & [K_{jj}]\end{bmatrix}\begin{Bmatrix}\{U\}\\ \{V\}\\ \{W\}\\ \{J\}\end{Bmatrix}=\begin{Bmatrix}\{F_u\}\\ \{F_v\}\\ \{F_w\}\\ \{F_j\}\end{Bmatrix}. \tag{47}$$

After assembling the contributions from all the elements, the global system of equations obtained can be written as:

$$[M]\{\ddot{\Delta}\}+[K]\{\Delta\}=\{F\}, \tag{48}$$

where $[M]$ is the mass matrix, $[K]$ the stiffness matrix, $\{F\}$ the load vector, and $\{\square\}$is the vector of nodal values of the generalized displacements.

Numerical results of the formulation presented above can be found in [23].

3. Finite Element Analysis of Plates with Embedded ActuatorsUsing FSDT

3.1 *Introduction*

The displacement fields of all equivalent single-layer plate theories are expanded in terms of the thickness coordinate up to a desired degree. However, theories higher than the third are not attempted due to very little improvement in accuracy for the amount of algebraic complexity and computational effort involved. Here we discuss the nonlinear finite element formulation of the first-order shear deformation plate theory (FSDT), which will be used in Phase II effort in conjunction with the layerwise theory of Reddy [14,15] to carry out the global-local analysis of composite laminates.

3.2 *Equations of motion*

The displacement field for the first-order shear deformation theory can be expressed in the form (see Reddy [15])

$$\begin{aligned} u(x,y,z,t) &= u_0(x,y,t) + z\phi_x(x,y,t) \\ v(x,y,z,t) &= v_0(x,y,t) + z\phi_y(x,y,t) \\ w(x,y,z,t) &= w_0(x,y,t) \end{aligned} \tag{49}$$

where (u_0, v_0, w_0) and (ϕ_x, ϕ_y) denote the displacements and rotations of transverse normals on the plane z = 0, respectively (see Figure 3).

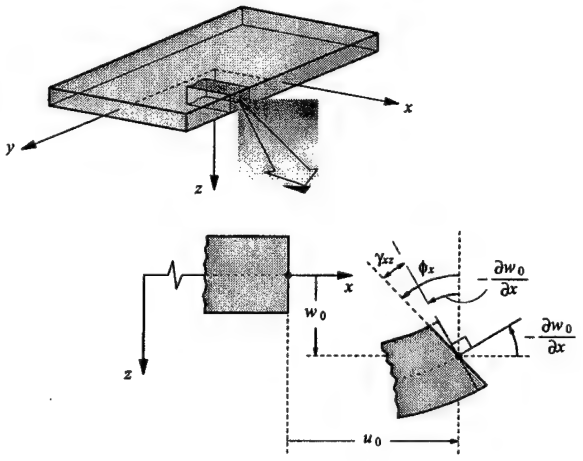

Figure 3. The kinematics of deformation of a typical edge in the first-order shear deformation plate theory (FSDT).

The equations of motion of the first-order shear deformation theory are derived using the dynamic version of the principle of virtual displacements (see Reddy [15]). The equations of motion are

$$\frac{\partial N_{xx}}{\partial x}+\frac{\partial N_{xy}}{\partial y}=I_0\frac{\partial^2 u_0}{\partial t^2}\,,\quad \frac{\partial N_{xy}}{\partial x}+\frac{\partial N_{yy}}{\partial y}=I_0\frac{\partial^2 v_0}{\partial t^2}\quad,$$

$$\frac{\partial Q_x}{\partial x}+\frac{\partial Q_y}{\partial y}+\mathrm{N}(u_0,v_0,w_0)+q=I_0\frac{\partial^2 w_0}{\partial t^2}\quad, \tag{50a}$$

$$\frac{\partial M_{xx}}{\partial x}+\frac{\partial M_{xy}}{\partial y}-Q_x=I_2\frac{\partial^2 \phi_x}{\partial t^2}\,,\quad \frac{\partial M_{xy}}{\partial x}+\frac{\partial M_{yy}}{\partial y}-Q_y=I_2\frac{\partial^2 \phi_y}{\partial t^2}\,,$$

where

$$\mathrm{N}(u_0,v_0,w_0)=\frac{\partial}{\partial x}\left(N_{xx}\frac{\partial w_0}{\partial x}+N_{xy}\frac{\partial w_0}{\partial y}\right)+\frac{\partial}{\partial y}\left(N_{xy}\frac{\partial w_0}{\partial x}+N_{yy}\frac{\partial w_0}{\partial y}\right) \tag{50b}$$

denotes the von Karman nonlinear contribution,

$$I_i=\sum_{k=1}^{N}\int_k^{k+1}\rho^{(k)}(z)^i\,dz\quad (i=0,1,2,...,6)\,, \tag{51}$$

are the mass inertias, and (N_{xx},N_{yy},N_{xy}) denote the total in-plane force resultants and (M_{xx},M_{yy},M_{xy}) the moment resultants:

$$\begin{Bmatrix}N_{xx}\\N_{yy}\\N_{xy}\end{Bmatrix}=\int_{-\frac{h}{2}}^{\frac{h}{2}}\begin{Bmatrix}\sigma_{xx}\\\sigma_{yy}\\\sigma_{xy}\end{Bmatrix}dz\,,\quad \begin{Bmatrix}M_{xx}\\M_{yy}\\M_{xy}\end{Bmatrix}=\int_{-\frac{h}{2}}^{\frac{h}{2}}\begin{Bmatrix}\sigma_{xx}\\\sigma_{yy}\\\sigma_{xy}\end{Bmatrix}z\,dz\,, \tag{52}$$

The force and moment resultants are related to the strains by

$$\begin{Bmatrix}\{N\}\\\{M\}\end{Bmatrix}=\begin{bmatrix}[A] & [B]\\[B] & [D]\end{bmatrix}\begin{Bmatrix}\{\varepsilon^{(0)}\}\\\{\varepsilon^{(1)}\}\end{Bmatrix}-\begin{Bmatrix}\{N^M\}\\\{M^M\}\end{Bmatrix},\qquad \{Q\}=[A]\{\gamma^{(0)}\}, \tag{53}$$

where

$$(A_{ij},B_{ij},D_{ij})=\sum_{k=1}^{N}\int_{z_k}^{z_{k+1}}\overline{Q}_{ij}^{(k)}(1,z,z^2)dz \tag{54}$$

and the stress resultants associated with the smart materials are defined by

$$\begin{Bmatrix}N_{xx}^M\\N_{yy}^M\\N_{xy}^M\end{Bmatrix}=\sum_{k=1}^{N}\int_{z_k}^{z_{k+1}}\begin{Bmatrix}\bar{e}_{31}\\\bar{e}_{32}\\\bar{e}_{36}\end{Bmatrix}^{(k)}H_z\,dz\,,\quad \begin{Bmatrix}M_{xx}^M\\M_{yy}^M\\M_{xy}^M\end{Bmatrix}=\sum_{k=1}^{N}\int_{z_k}^{z_{k+1}}\begin{Bmatrix}\bar{e}_{31}\\\bar{e}_{32}\\\bar{e}_{36}\end{Bmatrix}^{(k)}H_z\,z\,dz\,. \tag{55}$$

Here $\bar{e}_{ij}$ are the transformed moduli of the actuating/sensing material, and H_z is the electric field. The coefficients of A_{ij}, B_{ij} and D_{ij} are given in terms of the layer transformed stiffnesses $\bar{Q}_{ij}$ and layer coordinates z_{k+1} and z_k (see Figure 4).

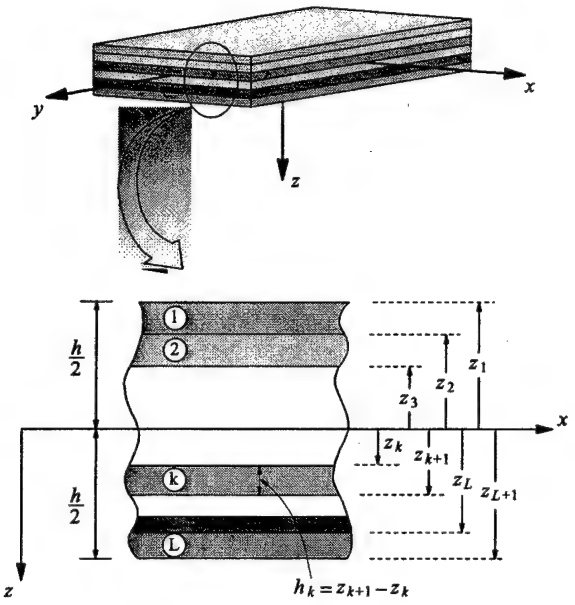

Figure 4. Schematic of a laminated plate.

3.3 *Velocity feedback control*

Here we consider the velocity proportional closed-loop feedback control, the magnetic field intensity H is expressed in terms of coil current $I(x,y,t)$ as

$$H(x,y,t) = k_c\, I(x,y,t)\,. \tag{56}$$

The current $I(x,y,t)$ is related to the transverse velocity of the plate $\dot{w}_0$ by

$$I(x,y,t) = c(t)\frac{\partial w_0}{\partial t}\,. \tag{57}$$

Here k_c denotes the coil constant, which can be expressed in terms of the coil width b_c, coil radius r_c and number of turns n_c in the coil by

$$k_c = \frac{n_c}{\sqrt{b_c^2 + 4r_c^2}}\,, \tag{58}$$

and $c(t)$ is the control gain. In this study the control gain is assumed to be constant. Hence it is represented as c.

3.4 *Weak formulation of the equations*

The weak forms of the equations of motion are

$$0=\int_{\Omega^e}\left\{\frac{\partial\delta u_0}{\partial x}N_{xx}+\frac{\partial\delta u_0}{\partial y}N_{xy}+\delta u_0\left[I_0\frac{\partial^2 u_0}{\partial t^2}\right]\right\}dxdy-\oint_\Gamma\{\delta u_0(N_{xx}\eta_x+N_{xy}\eta_y)\}ds\,,$$

$$0=\int_{\Omega^e}\left\{\frac{\partial\delta v_0}{\partial x}N_{xy}+\frac{\partial\delta v_0}{\partial y}N_{yy}+\delta v_0\left[I_0\frac{\partial^2 v_0}{\partial t^2}\right]\right\}dxdy-\oint_\Gamma\{\delta v_0(N_{xy}\eta_x+N_{yy}\eta_y)\}ds\,,$$

$$0=\int_{\Omega^e}\left\{\frac{\partial\delta\phi_y}{\partial x}M_{xy}+\frac{\partial\delta\phi_y}{\partial y}M_{yy}+\delta\phi_y Q_y+\delta\phi_y\left[I_2\frac{\partial^2\phi_y}{\partial t^2}\right]\right\}dxdy-\oint_\Gamma\delta\phi_y(M_{xy}n_x+M_{yy}n_y)ds\,,$$

$$0=\int_{\Omega^e}\left\{\frac{\partial\delta\phi_x}{\partial x}M_{xx}+\frac{\partial\delta\phi_x}{\partial y}M_{xy}+\delta\phi_x M_x+\delta\phi_x\left[I_2\frac{\partial^2\phi_x}{\partial t^2}\right]\right\}dxdy-\oint_\Gamma\delta\phi_x(M_{xx}n_x+M_{xy}n_y)ds\,,$$

$$0=\int_{\Omega^e}\left\{\frac{\partial\delta w_0}{\partial x}Q_x+\frac{\partial\delta w_0}{\partial y}Q_y-\delta w_0 q+\frac{\partial\delta w_0}{\partial x}\left(N_{xx}\frac{\partial w_0}{\partial x}+N_{xy}\frac{\partial w_0}{\partial y}\right)+\frac{\partial\delta w_0}{\partial y}\left(N_{xy}\frac{\partial w_0}{\partial x}+N_{yy}\frac{\partial w_0}{\partial y}\right)\right.$$
$$\left.+\delta w_0 I_0\frac{\partial^2 w_0}{\partial t^2}\right\}dxdy-\oint_\Gamma\delta w_o V_n ds\,, \qquad (59)$$

where V_n is defined as

$$V_n=\left(Q_x n_x+Q_y n_y\right)+\left(N_{xx}\frac{\partial w_0}{\partial x}+N_{xy}\frac{\partial w_0}{\partial y}\right)n_x+\left(N_{xy}\frac{\partial w_0}{\partial x}+N_{yy}\frac{\partial w_0}{\partial y}\right)n_y\,. \qquad (60)$$

3.5 *Finite element model*

The primary variables of the first-order theory are $u_n, u_s, w_0, \phi_n, \phi_s$, where (u_n, u_s) denotes in-plane normal and tangential displacements, and (ϕ_n, ϕ_s) are the rotations of a transverse line about the in-plane normal and tangent. Lagrange interpolation functions of $(u_n, u_s, w_0, \phi_n, \phi_s)$ are used for the formulation of the displacement finite element model. The finite element model has five degrees of freedom per node and four-node, eight-node, or nine-node rectangular elements may be used.

The generalized displacements are approximated over a typical element Ω^e by the expressions

$$u_x(x,y,t)=\sum_{i=1}^{m}u_i^e(t)\,\psi_i^e(x,y),\quad v_x(x,y,t)=\sum_{i=1}^{m}v_i^e(t)\,\psi_i^e(x,y)\,,$$

$$w_0(x,y,t)=\sum_{i=1}^{m}\overline{\Delta}_i^e(t)\,\varphi_i^e(x,y)\,, \qquad (61)$$

$$\phi_x(x,y,t)=\sum_{i=1}^{m}X_i^e(t)\,\psi_i^e(x,y),\quad \phi_y(x,y,t)=\sum_{i=1}^{m}Y_i^e(t)\,\psi_i^e(x,y)\,,$$

where ψ_i^e and φ_i^e denote the Lagrange interpolation functions. Here we chose the same approximation for the displacements (u_0, v_0, w_0) and rotations (ϕ_x, ϕ_y), although one could use different approximations for these two sets of fields.

The finite element model is of the compact form

$$\sum_{\beta=1}^{5}\sum_{j=1}^{n_\beta}\left(K_{ij}^{\alpha\beta}\Delta_j^\beta + C_{ij}^{\alpha\beta}\dot{\Delta}_j^\beta + M_{ij}^{\alpha\beta}\ddot{\Delta}_j^\beta\right) - F_i^\alpha = 0\ ,\ i=1,2,\ldots,n\,, \tag{62}$$

where $\alpha = 1, 2, 3, 4, 5$ and $n_1 = n_2 = n_3 = n_4 = n_5$. The nodal values Δ_j^β are

$$\Delta_j^1 = u_j,\ \Delta_j^2 = v_j,\ \Delta_j^3 = w_j,\ \Delta_j^4 = X_j,\ \Delta_j^5 = Y_j \tag{63}$$

and the non-zero stiffness, mass, and damping coefficients are defined in Appendix I.

This completes the general non-linear finite element model development for the first-order shear deformation plate theory with actuator layers. The finite element model is called a displacement finite element model because it is based on equations of motion expressed in terms of the displacements, and the generalized displacements are the primary nodal degrees of freedom.

Transient Analysis

Here we discuss the procedures to determine the transient response of composite laminates. The equations of motion (62) must be approximated further using the Newmark method. First, note that Eq. (62) has the general form

$$[M^e]\{\ddot{u}^e\} + [C^e]\{\dot{u}^e\} + [K^e]\{u^e\} = \{F^e\} \tag{64}$$

The global displacement vector $\{u\}$ is subject to the initial conditions that the displacement and velocity are known at time $t = 0 : \{u(0)\} = \{u\}_0 \quad \{\dot{u}(0)\} = \{\dot{u}\}_0$. In Newmark's scheme, the function (of time) and its first derivative are approximated using Taylor's series and only terms up to the second derivative are included:

$$\{u\}_{s+1} = \{u\}_s + \Delta t\{\dot{u}\}_s + \frac{1}{2}(\Delta t)^2\{\ddot{u}\}_{s+\gamma},\quad \{\dot{u}\}_{s+1} = \{\dot{u}\}_s + \Delta t\{\ddot{u}\}_{s+\alpha},\quad \{\ddot{u}\}_{s+\alpha} = (1-\alpha)\{\ddot{u}\}_s + \alpha\{\ddot{u}\}_{s+1} \tag{65}$$

where Δt is the time increment, $\Delta t = t_{s+1} - t_s$ and t_s is the current time and t_{s+1} is the next time at which we seek the solution. We assume that the solution at time t_s is known. Substituting the third equation into the first two and solving for $\{\ddot{u}\}$, we obtain

$$\{\dot{u}\}_{s+1} = \{\dot{u}\}_s + a_1\{\ddot{u}\}_s + a_2\{\ddot{u}\}_{s+1}\ ,\quad \{\ddot{u}\}_{s+1} = a_3\left(\{u\}_{s+1} - \{u\}_s\right) - a_4\{\dot{u}\}_s - a_5\{\ddot{u}\}_s \tag{66}$$

$$a_1 = (1-\alpha)\Delta t\,,\ a_2 = \alpha\Delta t\,,\ a_3 = \frac{2}{\gamma(\Delta t)^2},\ a_4 = a_3\Delta t\,,\ a_5 = \frac{(1-\gamma)}{\gamma}, \tag{67}$$

and α and γ are parameters that determine the stability and accuracy of the scheme Finally ,we obtain the finite element equations of the form

$$[\hat{K}]_{s+1}\{\Delta\}_{s+1} = \{\hat{F}\}_{s;s+1} \tag{68}$$

$$[\hat{K}]_{s+1} = [K]_{s+1} + a_3[M]_{s+1} + a_6[C]_{s+1},\quad \{\hat{F}\}_{s,s+1} = \{F\}_{s+1} + [M]_{s+1}\{A\}_s + [C]_{s+1}\{B\}_s$$

$$\{A\}_s = a_3\{u\}_s + a_4\{\dot{u}\}_s + a_5\{\ddot{u}\}_s,\qquad \{B\}_s = a_6\{u\}_s + a_7\{\dot{u}\}_s + a_8\{\ddot{u}\}_s \tag{69}$$

$$a_6 = \frac{2\alpha}{\gamma\Delta t},\ a_7 = \frac{2\alpha}{\gamma} - 1,\ a_8 = \Delta t\left(\frac{\alpha}{\gamma} - 1\right) \tag{70}$$

3.6 Numerical results - linear

Numerical studies are carried out to analyze the vibration suppression characteristics for the different lamination schemes and boundary conditions using the previously developed TSDT finite element models. The baseline of the simulations is the simply supported square laminate ($a/b = 1$, $a/h = 10$) under sinusoidal distributions of velocity initial conditions over the domain, $\frac{\partial w}{\partial t}(x, y, t = 0) = \sin\frac{\pi x}{a}\sin\frac{\pi y}{b}$. The selected time step in the present study is 0.0005sec. The lamination scheme $(\theta_1, \theta_2, \theta_3, \theta_4, m)_s$ means that the 10 layered symmetric laminate with the fiber orientation being $(\theta_1, \theta_2, \theta_3, \theta_4, m, m, \theta_4, \theta_3, \theta_2, \theta_1)$, where m stands for the magnetostrictive layer and subscript s stands for symmetric. The material properties of Terfenol-D and the elastic composite materials are listed in Table 1.

In finite element analysis, solution symmetries should be taken advantage of identifying the computational domain because they reduce computational efforts. For a laminated composite plate with all edges simply-supported or clamped, a quadrant of the plate may be used as the computational domains. Figure 5 shows the two types of simply supported boundary condition for third-order shear deformation theory. Quarter plate models with proper boundary conditions can be used in the antisymmetric laminates with simply supported boundary condition but not with the clamped cases. For symmetric laminates, the simply supported cross-ply laminates can be modeled as a quarter plate.

Table 1. Material properties of magnetostrictive and elastic composite materials.

Material	E_1 $[GPa]$	E_2 $[GPa]$	G_{13} $[GPa]$	G_{23} $[GPa]$	G_{12} $[GPa]$	ν_{12}	ρ $[Kg\,m^{-3}]$	D_k $[10^{-8}\,mA^{-1}]$
Terfenol-D	26.5	26.5	13.25	13.25	13.25	0	9250	1.67
CFRP	138.6	8.27	4.96	4.12	4.96	0.26	1824	-
Gr-Ep(AS)	137.9	8.96	7.20	6.21	7.20	0.30	1450	-
Gl-Ep	53.78	17.93	8.96	3.45	8.96	0.25	1900	-
Br-Ep	206.9	20.69	6.9	4.14	6.9	0.30	1950	-

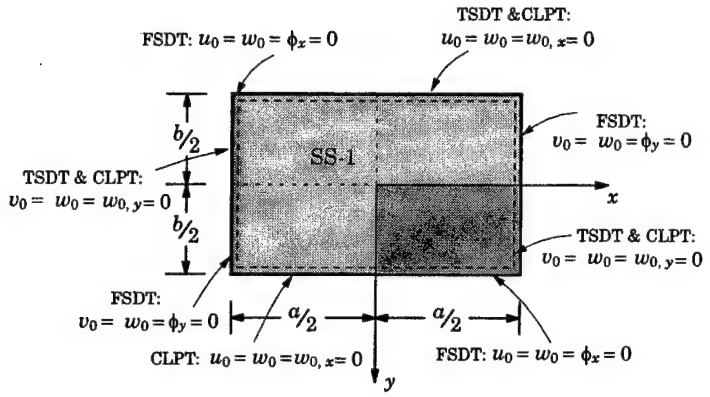

Figure 5. Simply supported boundary conditions, SS-1and SS-2, for laminates using the third-order shear deformation theory.

Simply supported composite laminates

To compare with the analytical results, the SS-1 boundary conditions and quarter plate F.E. model have been used in the symmetric cross-ply laminates. The vibration suppression effects from the analytical and numerical methods are within the reasonable range of distribution as shown in Figure 6. Figure 7 shows the central displacements using the different plate theories (CLPT, FSDT, and TSDT) for two different lamination schemes. It is observed that CLPT gives the higher vibration suppression capacity in both cases. This is expected because the CLPT renders the plate stiffer compared to the other theories. After studying the influence of lamina material properties on the amplitude of vibration and vibration suppression times, it is observed that materials having the almost same E_1/E_2 ratio have similar vibration suppression characteristics. Figure 8 shows the vibration suppression characteristics for the different laminate materials.

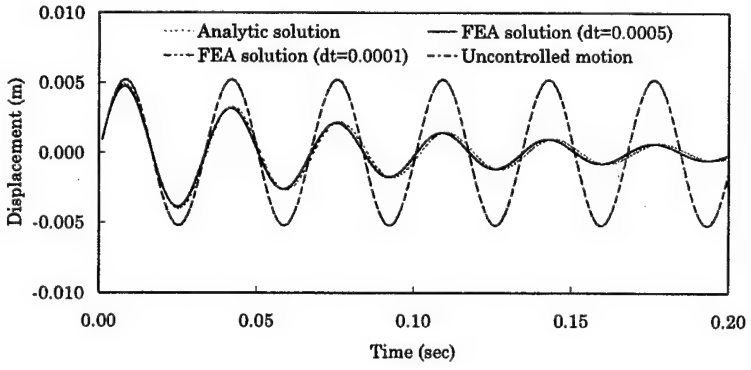

Figure 6. Comparison of analytical and numerical central displacements with the case of uncontrolled behaviour for the symmetric cross-ply CFRP laminates $(m,90,0,90,0)_s$.

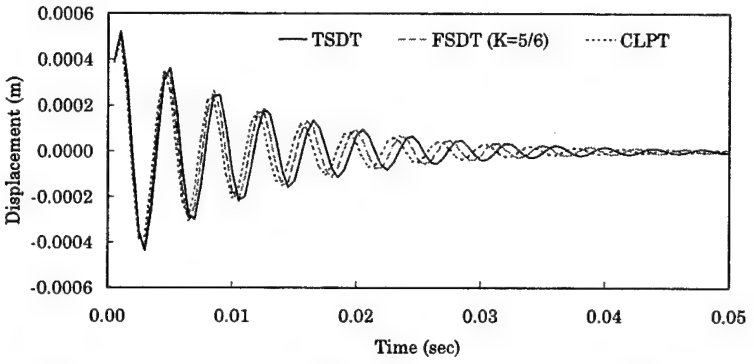

Figure 7(a) The comparison of the central displacements by the different plate theories for CFRP simply supported laminates; symmetric cross-ply CFRP laminate $(m,90,0,90,0)_s$.

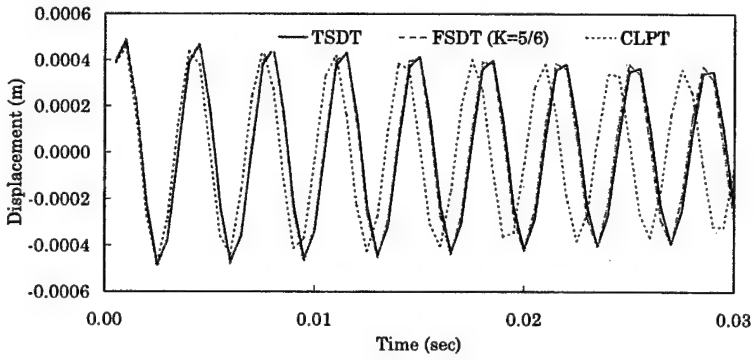

(b)

Figure 7(b). The comparison of the central displacements by the different plate theories for CFRP simply supported laminates; symmetric cross-ply CFRP laminate $(0,90,0,90,m)_s$.

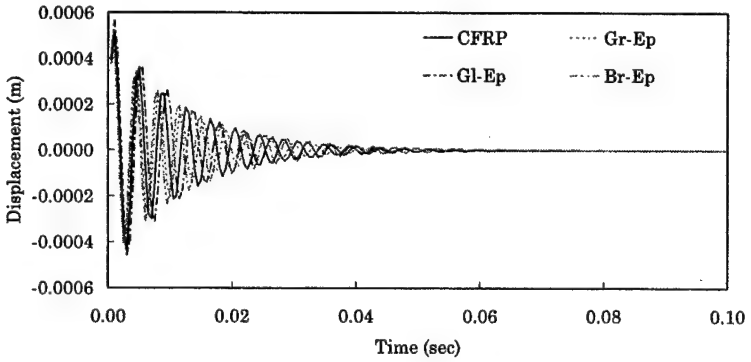

Figure 8. The effect of the lamina material properties on the vibration suppression characteristics for the symmetric cross-ply laminates $(m,90,0,90,0)_s$.

Clamped composite laminates

The same laminated plates but with fully clamped boundary conditions are analyzed using a 8×8 mesh in a full plate. The effect of the boundary conditions on the vibration characteristic is shown in the Figure 9. The maximum displacements of the simply supported plate are greater than those of the clamped case, which is expected. For the vibration suppression, the cases of simply supported laminates that has the bigger displacements take less suppression time.

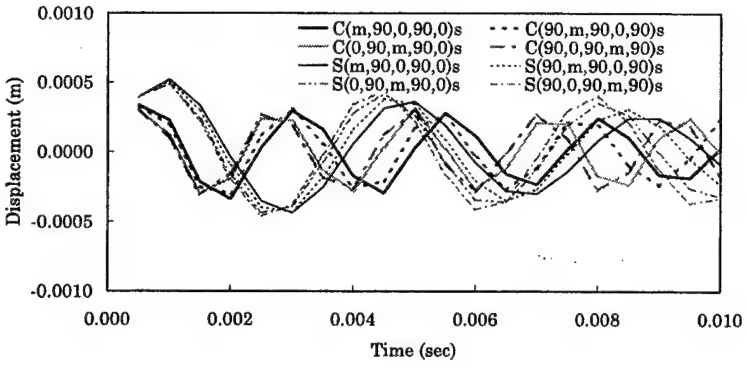

Figure 9. The effect of boundary conditions on the central displacements for the different laminates; comparison of simply supported and clamped laminates.

Effects of the mechanical loading

Numerical studies are also carried out to analyze the vibration suppression characteristics for the composite laminates under the uniformly distributed load q_0 instead of velocity initial conditions. Figure 10 shows the vibration suppressions for the selected simply supported and clamped laminated plates under continuously applied uniformly distributed loading while Figure 11 shows the case under suddenly applied and removed distributed loading. The effect of sinusoidal loading on the central displacement has been studied. The results of the symmetric cross-ply laminate with simply supported laminates subjected to the sinusoidal and uniformly distributed loadings are shown in Figure 12. Here the sinusoidal loading is $\sin\frac{\pi x}{a}\sin\frac{\pi y}{b}$ and the transverse displacements in Figures 10-12 are plotted in the nondimensionalized forms as $w_0\,(100)\frac{E_2 h^3}{b^4 q_0}$.

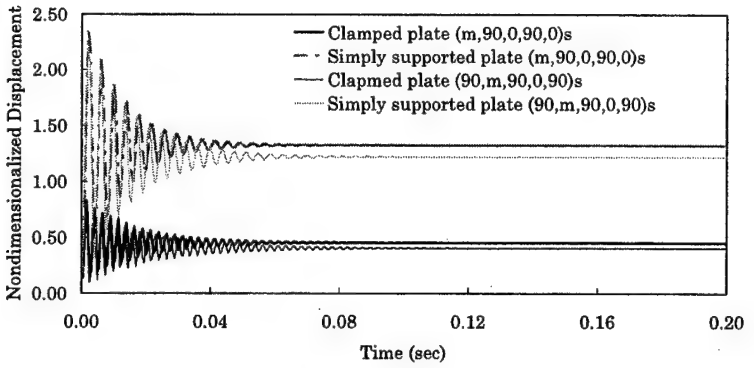

Figure 10. Nondimensionalized central displacement for simply supported and clamped laminated plates under uniformly distributed loading.

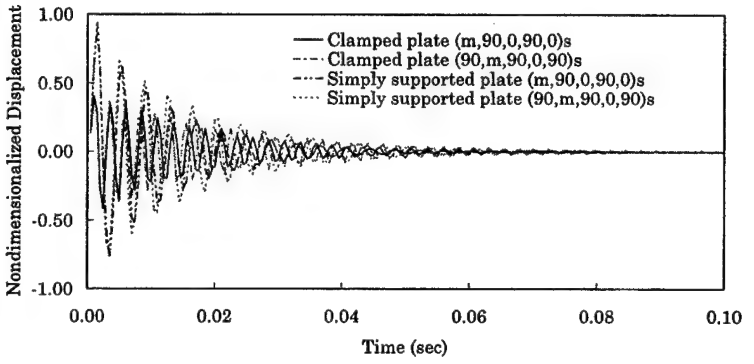

Figure 11. Nondimensionalized central displacement for simply supported and clamped laminated plates under suddenly applied uniformly distributed loading.

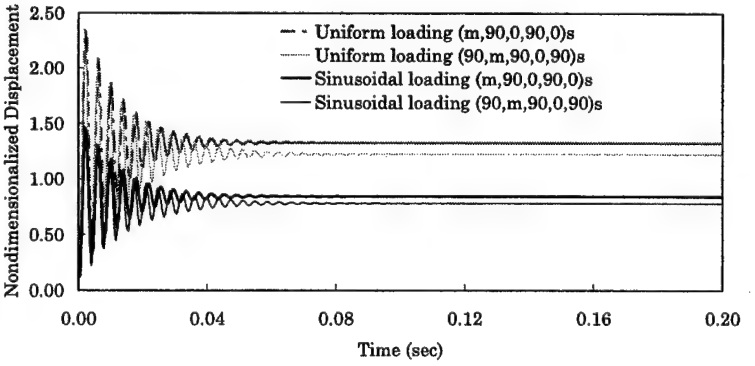

Figure 12. Comparison of central displacements for simply supported laminated plates under Sinusoidal and uniformly distributed loadings.

3.7 Numerical results - nonlinear

Laminated composite square plate $(a/b=1)$ with both the upper and lower surfaces embedded magnetostrictive materials, as shown in Figure 2, is considered. The plate is made of composite fiber reinforced polymer (CFRP) composites and the magnetostrictive material, Terfenol-D. The adhesive layers are neglected in the analysis. The laminated composite plates are composed of total 10 layers and all the layers are assumed to be of the same thickness. Two side-to-thickness ratios $a/h=10$ and 100 are considered to represent the thick and thin composite plates.

The geometric and material parameters used are

- Geometry : $a=b=100cm,\quad h=10\ or\ 1cm$
- CFRP : $E_1=138.6\ GPa, E_2=8.27\ GPa, G_{12}=G_{13}=4.96GPa, G_{23}=4.12GPa$
  $\nu_{12}=0.26,\ \rho=1824\,Kg/m^3$
- Terfenol-D : $E^m=26.5\ GPa, d^m=1.67\times10^{-8}\,mA^{-1}, \nu=0,\ \rho=9250\,Kg/m^3$

The numerical analysis variables in this study and the representing notations that are used in the result figures are the following:

- 3 Plate theories : CLPT***(C)***, FSDT***(F)***, TSDT***(T)***
- 4 Lamination schemes : symmetric cross-ply $(\mathrm{m},90,0,90,0)\mathrm{s}$ ***(SC)***,symmetric angle-ply
  $(\mathrm{m},45,-45,45,-45)\mathrm{s}$ ***(SA)***, symmetric general angle-ply
  $(\mathrm{m},45,-45,0,90)\mathrm{s}$ ***(SG)***, and asymmetric general angle-ply
  $(\mathrm{m},45,-45,15,-15,0,90,30,-30,\mathrm{m})$ ***(AS)*** laminated plates.
- 4 Loading conditions : Uniformly distributed load***(UMD)***, uniformly distributed impact load***(IMD)***, uniformly distributed sinusoidal load***(SUMD)***, uniformly distributed sinusoidal impact load***(SIMD)***.
- The other indices: Linear***(L)*** and Nonlinear***(NL)*** analyses, Thick$(a/h=10)$ plate***(10)*** and thin$(a/h=100)$ plate***(100)***, and Load intensity $q_0=10^0$ ***(E0)***, $q_0=5.0\times10^7$ ***(5E7)***, and so on.

The shear correction factor used in FSDT is 5/6; m represents magnetostrictive layer and subscript s stands for symmetric, and the sinusoidal load means

$$q(x,y)=q_0\sin(\pi x/a)\sin(\pi y/b).$$

The displacements are measured at the center of the plates and nondimensionalized as $\bar{w}_c=100\times w_0 E_2h^3/a^4q_0$. A tolerance of $\varepsilon=10^{-2}$ is used for convergence in the Newton-Raphson iteration scheme to check for convergence of the nodal displacements.

First, the effects of the different plate theories on the transient responses are considered. Linear and nonlinear responses obtained by the three different theories are presented in Figure 13. It is observed that the effect of nonlinearity on the transient responses is to decrease the amplitude and increase the frequency. Note that due to the large geometric nonlinearity effects the nonlinear transient behaviors between TSDT and other two theories are apparent. It is also observed that the CLPT theory gives higher frequencies and lower amplitudes. It is because CLPT theory renders the plate stiffer compared to the other two theories.

Next, the effect of applied loading conditions on the vibration suppression can be seen from the Figure 14. The four different loading conditions are considered to study their effect on the response. They are uniformly distributed load, uniformly distributed sinusoidal load, uniformly distributed impact load and uniformly distributed sinusoidal impact load. Since the first two loadings are continuously applied over the computational domain during the analysis the converged transient solution is different for each case. The plots show the differences between the loading conditions on transient response effects for the different lamination schemes.

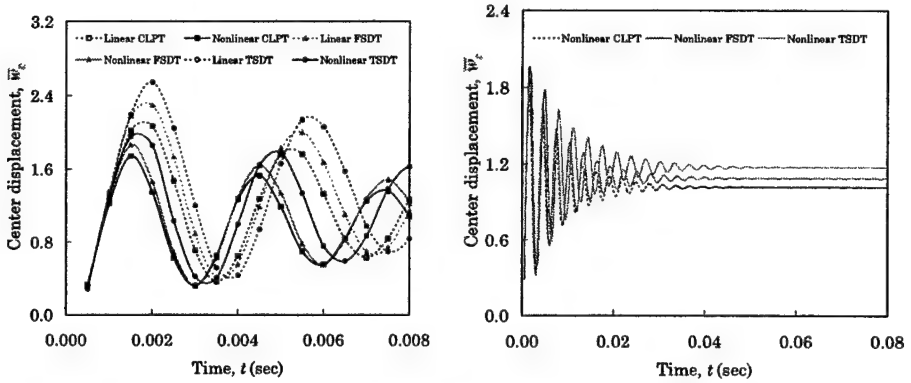

Figure 13. Effects of plate theories on the nonlinear transient responses for the symmetric cross-ply thick (a/h =10) laminates with SSSS boundary conditions and under uniformly distributed load ($q_0 = 5\times10^7$).

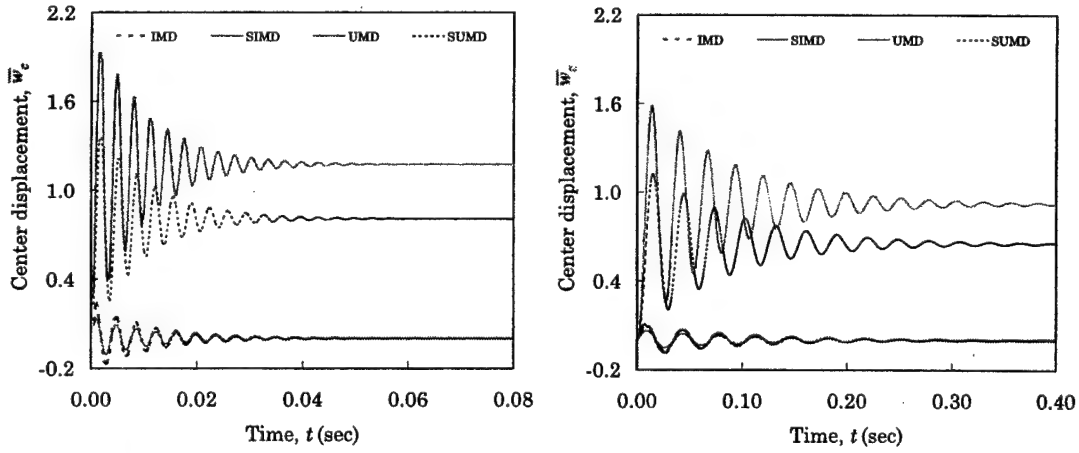

(a) Sym. cross-ply laminate (a/h=10)

(b) Sym. cross-ply laminate(a/h=100)

Figure 14(a,b). Effects of loading conditions (Impact), Uniformly distributed loading on the transient responses with SSSS boundary conditions (cross-ply laminates).

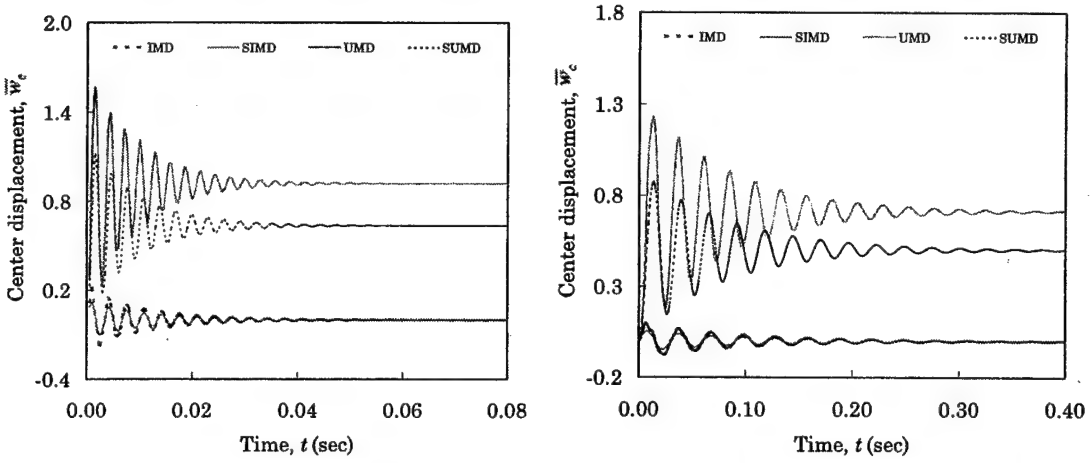

(c) Sym. angle-ply laminate (a/h=10)

(d) Sym. angle-ply laminate (a/h=100)

Figure 14(c,d). Effects of loading conditions (Impact), Uniformly distributed loading] on the transient responses with SSSS boundary conditions (angle-ply laminates).

CONCLUSIONS

The development of physically-based damage models and nonlinear-finite models based on the first–order shear deformation theory and the computer implementation of the nonlinear finite element model were the major accomplishments of the study. The integration of these elements into the layerwise theory for global-local analysis and prediction of damage and failures in composite laminates can be carried out. The effects of the lamination scheme, types of load, and boundary conditions on the static and dynamic deflection was investigated. It is observed that the effect of nonlinearity on the transient responses is to decrease the amplitude and increase the frequency of nondimensionalized center displacement. It so also observed that the nonlinear transient behaviors between TSDT and other two theories (CLPT and FSDT) are apparent because of the geometric nonlinearity.

RELATIONSHIP TO FUTURE RESEARCH AND DEVELOPMENT

The integration of physically based damage models that account for micros-scale as well as damage into robust computational models is perhaps the most significant contribution of this research. From the science and technology points of view, the results of this research will contribute to a fundamental understanding of the non-linear behavior and damage progression in thick composite and sandwich structures with embedded sensors and actuators. The results will also have a significant impact on the design of composite structures used in lightweight composite and sandwich structural components used in army and marine structures.

Acknowledgements

The author gratefully acknowledges the technical contributions reported herein by S. J. Lee, J. E. Semedo Garção, and Donald H. Robbins, Jr.

REFERENCES

1. Krajcinovic, D., "Constitutive theories for solids with defective microstructure," *Damage Mechanics and Continuum Modeling*, N. Stubbs and D. Krajcinovic (eds.), American Society of Civil Engineers, New York, pp. 39-56, 1985.
2. Krajcinovic, D., *Damage Mechanics*, North-Holland, Amsterdam, 1996.
3. Chang, F. K. and Chang, K. Y., "A progressive damage model for laminated composites containing stress concentrations," *Journal of Composite Materials*, **21**, pp. 834-855, 1987.
4. Aboudi, J., "damage in composites - modeling of imperfect bonding," *Composites Science and Technology*, **28**, pp. 103-128, 1987.
5. Ladeveze, P. and Le Dantec, E., "Damage modeling of the elementary ply for laminated composites," *Composites Science and Technology*, **43**, pp. 257-267, 1992.
6. Fish, J., Yu, Q., and Shek, K., "Computational damage mechanics for composite materials based on mathematical homogenization," *Int. J. Numer. Meth. Engng.*, **45**, pp.1657-1679, 1999.
7. Ghosh, S., Lee, K., and Moorthy, S., "Multiple scale analysis of heterogeneous elastic structures using homogenization theory and voronoi cell finite element method," *Int. J. Solids Struct.*, **32**, pp. 27-62, 1995.
8. Ghosh, S., Lee, K, and Moorthy, S. "Two scale analysis of heterogeneous elastic-plastic materials with asymptotic homogenization and voronoi cell finite element model", *Comput. Methods Appl. Mech. Engng.*, **132**, pp. 63-116, 1996.
9. Lee, K., Moorthy, S., and Ghosh, S., "Multiple scale computational model for damage in composite materials," *Comput. Methods Appl. Mech. Engng.*, **172**, pp. 175-201, 1999.
10. Skrzypek, J., and Ganczarski, A., *Modeling of Material Damage and Failure of Structures*, Springer, Berlin, 1999.
11. Barbero, E., and De Vivo, L., "A constitutive model for elastic damage in fiber-reinforced PMC laminae," *Int. Journal of Damage Mechanics*, **10**, pp. 73-93, 2001.
12. Cordebois, J. P., and Sidoroff, F., "Damage induced elastic anisotropy," *Mechanical Behavior of Anisotropic Solids*, J. P. Boehler (ed.), Martinus Nijhoff, The Hague, pp. 761-774, 1982.
13. Ochoa, O. O., and Reddy, J. N., *Finite Element Analysis of Composite Laminates*, Kluwer Academic Publishers, Dordrecht, The Netherlands, 1992.
14. Reddy, J. N., "A generalization of two-dimensional theories of laminated composite plates,". *Commun. Appl. Numer. Meth.*, **3**, pp. 173-180, 1987.
15. Reddy, J. N., *Mechanics of Laminated Composite Plates: Theory and Analysis*, CRC Press, Boca Raton, Florida, 1997.
16. Robbins, D. H., and Reddy, J. N., "Modeling of thick composites using a layer-wise laminate theory," *International Journal for Numerical Methods in Engineering*, **36**, pp. 655-677, 1993.
17. Reddy, J. N. and Mitchell, J. A., "Refined Nonlinear Theories of Laminated Composite Structures with Piezoelectric Laminae", *Sadhana* (Journal of the Indian Academy of Sciences), **20**(2-4), pp. 721-747, 1995.
18. Saravanos, D. A., Heyliger, P. R., Hopkins, D. A., "Layerwise mechanics and finite element for the dynamic analysis of piezoelectric composite plates", *International Journal of Solids and Structures*, **34**(3) 359-378, 1997.
19. Garção, J. E. S., "A closed form solution for the analysis of simply supported piezolaminated plates", Report G01/02, Project POCTI / EME / 37559/2001, IDMEC-IST, 2002.
20. Bisegna, P., and Maceri, F., "An exact three-dimensional solution for simply supported rectangular piezoelectric plates", *Journal of Applied Mechanics*, **63**, 628-638, 1996.
21. Heyliger, P. R., "Exact solutions for simply supported laminated piezoelectric plates", *Journal of Applied Mechanics*, **64**, 299-306, 1997.

22. Reddy, J. N. and Krishnan, S., "Vibration Control of Laminated Plates Using Embedded Smart Layers," *Structural Engineering and Mechanics*, **12**(2), pp. 135-156, 2001.
23. Semedo Garcão, J. E., Mota Soares, C. M., Mota Soares, C. A., and Reddy, J. N., ``Analysis of Adaptive Laminated Plate Structures Using Layerwise Finite Element Models," *Computers and Structures* (to appear).

APPENDIX I: FINITE ELEMENT COEFFICIENTS

$$K_{ij}^{11} = \int_{\Omega^e}\left[A_{11}\frac{\partial\psi_i}{\partial x}\frac{\partial\psi_j}{\partial x} + A_{66}\frac{\partial\psi_i}{\partial y}\frac{\partial\psi_j}{\partial y} + A_{16}\left(\frac{\partial\psi_i}{\partial x}\frac{\partial\psi_j}{\partial y} + \frac{\partial\psi_i}{\partial y}\frac{\partial\psi_j}{\partial x}\right)\right]dxdy\,,$$

$$K_{ij}^{12} = \int_{\Omega^e}\left(A_{12}\frac{\partial\psi_i}{\partial x}\frac{\partial\psi_j}{\partial y} + A_{16}\frac{\partial\psi_i}{\partial x}\frac{\partial\psi_j}{\partial x} + A_{26}\frac{\partial\psi_i}{\partial y}\frac{\partial\psi_j}{\partial y} + A_{66}\frac{\partial\psi_i}{\partial y}\frac{\partial\psi_j}{\partial x}\right)dxdy\,,$$

$$(K_{NL}^{13})_{ij} = \int_{\Omega^e}\left\{\frac{1}{2}\left[\left(A_{11}\frac{\partial w_0}{\partial x}\frac{\partial\psi_i}{\partial x}\frac{\partial\varphi_j}{\partial x} + A_{12}\frac{\partial w_0}{\partial y}\frac{\partial\psi_i}{\partial x}\frac{\partial\varphi_j}{\partial y} + A_{16}\left(\frac{\partial w_0}{\partial x}\frac{\partial\psi_i}{\partial x}\frac{\partial\varphi_j}{\partial y} + \frac{\partial w_0}{\partial y}\frac{\partial\psi_i}{\partial x}\frac{\partial\varphi_j}{\partial x}\right)\right)\right.\right.$$
$$\left.\left. + \left(A_{16}\frac{\partial w_0}{\partial x}\frac{\partial\psi_i}{\partial y}\frac{\partial\varphi_j}{\partial x} + A_{26}\frac{\partial w_0}{\partial y}\frac{\partial\psi_i}{\partial y}\frac{\partial\varphi_j}{\partial y} + A_{66}\left(\frac{\partial w_0}{\partial x}\frac{\partial\psi_i}{\partial y}\frac{\partial\varphi_j}{\partial y} + \frac{\partial w_0}{\partial y}\frac{\partial\psi_i}{\partial y}\frac{\partial\varphi_j}{\partial x}\right)\right)\right]\right\}dxdy$$

$$K_{ij}^{14} = \int_{\Omega^e}\left[B_{11}\frac{\partial\psi_i}{\partial x}\frac{\partial\psi_j}{\partial x} + B_{66}\frac{\partial\psi_i}{\partial y}\frac{\partial\psi_j}{\partial y} + B_{16}\left(\frac{\partial\psi_i}{\partial x}\frac{\partial\psi_j}{\partial y} + \frac{\partial\psi_i}{\partial y}\frac{\partial\psi_j}{\partial x}\right)\right]dxdy\,,$$

$$K_{ij}^{15} = \int_{\Omega^e}\left(B_{12}\frac{\partial\psi_i}{\partial x}\frac{\partial\psi_j}{\partial y} + B_{16}\frac{\partial\psi_i}{\partial x}\frac{\partial\psi_j}{\partial x} + B_{26}\frac{\partial\psi_i}{\partial y}\frac{\partial\psi_j}{\partial y} + B_{66}\frac{\partial\psi_i}{\partial y}\frac{\partial\psi_j}{\partial x}\right)dxdy\,,$$

$$K_{ij}^{21} = \int_{\Omega^e}\left(A_{16}\frac{\partial\psi_i}{\partial x}\frac{\partial\psi_j}{\partial x} + A_{66}\frac{\partial\psi_i}{\partial x}\frac{\partial\psi_j}{\partial y} + A_{12}\frac{\partial\psi_i}{\partial y}\frac{\partial\psi_j}{\partial x} + A_{26}\frac{\partial\psi_i}{\partial y}\frac{\partial\psi_j}{\partial y}\right)dxdy\,,$$

$$K_{ij}^{22} = \int_{\Omega^e}\left[A_{22}\frac{\partial\psi_i}{\partial y}\frac{\partial\psi_j}{\partial y} + A_{66}\frac{\partial\psi_i}{\partial x}\frac{\partial\psi_j}{\partial x} + A_{26}\left(\frac{\partial\psi_i}{\partial x}\frac{\partial\psi_j}{\partial y} + \frac{\partial\psi_i}{\partial y}\frac{\partial\psi_j}{\partial x}\right)\right]dxdy\,,$$

$$(K_{NL}^{23})_{ij} = \int_{\Omega^e}\left\{\frac{1}{2}\left[\left(A_{12}\frac{\partial w_0}{\partial x}\frac{\partial\psi_i}{\partial y}\frac{\partial\varphi_j}{\partial x} + A_{22}\frac{\partial w_0}{\partial y}\frac{\partial\psi_i}{\partial y}\frac{\partial\varphi_j}{\partial y} + A_{26}\left(\frac{\partial w_0}{\partial x}\frac{\partial\psi_i}{\partial y}\frac{\partial\varphi_j}{\partial y} + \frac{\partial w_0}{\partial y}\frac{\partial\psi_i}{\partial y}\frac{\partial\varphi_j}{\partial x}\right)\right)\right.\right.$$
$$\left.\left. + \left(A_{16}\frac{\partial w_0}{\partial x}\frac{\partial\psi_i}{\partial x}\frac{\partial\varphi_j}{\partial x} + A_{26}\frac{\partial w_0}{\partial y}\frac{\partial\psi_i}{\partial x}\frac{\partial\varphi_j}{\partial y} + A_{66}\left(\frac{\partial w_0}{\partial x}\frac{\partial\psi_i}{\partial x}\frac{\partial\varphi_j}{\partial y} + \frac{\partial w_0}{\partial y}\frac{\partial\psi_i}{\partial x}\frac{\partial\varphi_j}{\partial x}\right)\right)\right]\right\}dxdy$$

$$K_{ij}^{24} = \int_{\Omega^e}\left(B_{16}\frac{\partial\psi_i}{\partial x}\frac{\partial\psi_j}{\partial x} + B_{66}\frac{\partial\psi_i}{\partial x}\frac{\partial\psi_j}{\partial y} + B_{12}\frac{\partial\psi_i}{\partial y}\frac{\partial\psi_j}{\partial x} + B_{26}\frac{\partial\psi_i}{\partial y}\frac{\partial\psi_j}{\partial y}\right)dxdy\,,$$

$$K_{ij}^{25} = \int_{\Omega^e}\left[B_{22}\frac{\partial\psi_i}{\partial y}\frac{\partial\psi_j}{\partial y} + B_{66}\frac{\partial\psi_i}{\partial x}\frac{\partial\psi_j}{\partial x} + B_{26}\left(\frac{\partial\psi_i}{\partial x}\frac{\partial\psi_j}{\partial y} + \frac{\partial\psi_i}{\partial y}\frac{\partial\psi_j}{\partial x}\right)\right]dxdy\,,$$

$$(K_{NL}^{31})_{ij} = \int_{\Omega^e}\left\{\frac{\partial\psi_i}{\partial x}\left[\frac{\partial w_0}{\partial x}\left(A_{11}\frac{\partial\psi_j}{\partial x} + A_{16}\frac{\partial\psi_j}{\partial y}\right) + \frac{\partial w_0}{\partial y}\left(A_{16}\frac{\partial\psi_j}{\partial x} + A_{66}\frac{\partial\psi_j}{\partial y}\right)\right]\right.$$
$$\left. + \frac{\partial\psi_i}{\partial y}\left[\frac{\partial w_0}{\partial x}\left(A_{16}\frac{\partial\psi_j}{\partial x} + A_{66}\frac{\partial\psi_j}{\partial y}\right) + \frac{\partial w_0}{\partial y}\left(A_{12}\frac{\partial\psi_j}{\partial x} + A_{26}\frac{\partial\psi_j}{\partial y}\right)\right]\right\}dady$$

$$(K_{NL}^{32})_{ij} = \int_{\Omega^e}\left\{\frac{\partial\psi_i}{\partial x}\left[\frac{\partial w_0}{\partial x}\left(A_{12}\frac{\partial\psi_j}{\partial y}+A_{16}\frac{\partial\psi_j}{\partial x}\right)+\frac{\partial w_0}{\partial y}\left(A_{26}\frac{\partial\psi_j}{\partial y}+A_{66}\frac{\partial\psi_j}{\partial x}\right)\right]\right.$$
$$\left.+\frac{\partial\psi_i}{\partial y}\left[\frac{\partial w_0}{\partial x}\left(A_{26}\frac{\partial\psi_j}{\partial y}+A_{66}\frac{\partial\psi_j}{\partial x}\right)+\frac{\partial w_0}{\partial y}\left(A_{22}\frac{\partial\psi_j}{\partial y}+A_{26}\frac{\partial\psi_j}{\partial x}\right)\right]\right\}dady$$

$$K_{ij}^{33} = \int_{\Omega^e}\left\{\frac{\partial\varphi_i}{\partial x}\left(A_{45}\frac{\partial\varphi_j}{\partial y}+A_{55}\frac{\partial\varphi_j}{\partial x}\right)+\frac{\partial\varphi_i}{\partial y}\left(A_{44}\frac{\partial\varphi_j}{\partial y}+A_{45}\frac{\partial\varphi_j}{\partial x}\right)\right\}dxdy\,,$$

$$(K_{NL}^{33})_{ij}^{(2)} = \left(\frac{1}{2}\right)\int_{\Omega^e}\left\langle\frac{\partial\psi_i}{\partial x}\left\{\left[\left[A_{11}\left(\frac{\partial w_0}{\partial x}\right)^2\frac{\partial\varphi_j}{\partial x}+A_{12}\frac{\partial w_0}{\partial x}\frac{\partial w_0}{\partial y}\frac{\partial\varphi_j}{\partial y}+A_{16}\left(\left(\frac{\partial w_0}{\partial x}\right)^2\frac{\partial\varphi_j}{\partial y}+\frac{\partial\varphi_j}{\partial x}\frac{\partial w_0}{\partial x}\frac{\partial w_0}{\partial y}\right)\right]\right]\right.\right.$$
$$\left.+\left\{\left[A_{16}\frac{\partial w_0}{\partial x}\frac{\partial w_0}{\partial y}\frac{\partial\varphi_j}{\partial x}+A_{26}\left(\frac{\partial w_0}{\partial y}\right)^2\frac{\partial\varphi_j}{\partial y}+A_{66}\left(\frac{\partial w_0}{\partial x}\frac{\partial w_0}{\partial y}\frac{\partial\varphi_j}{\partial y}+\frac{\partial\varphi_j}{\partial x}\left(\frac{\partial w_0}{\partial y}\right)^2\right)\right]\right\}\right]$$
$$+\frac{\partial\psi_i}{\partial y}\left\{\left[\left[A_{16}\left(\frac{\partial w_0}{\partial x}\right)^2\frac{\partial\varphi_j}{\partial x}+A_{26}\frac{\partial w_0}{\partial x}\frac{\partial w_0}{\partial y}\frac{\partial\varphi_j}{\partial y}+A_{66}\left(\left(\frac{\partial w_0}{\partial x}\right)^2\frac{\partial\varphi_j}{\partial y}+\frac{\partial\varphi_j}{\partial x}\frac{\partial w_0}{\partial x}\frac{\partial w_0}{\partial y}\right)\right]\right]\right.$$
$$\left.\left.+\left\{\left[A_{12}\frac{\partial w_0}{\partial x}\frac{\partial w_0}{\partial y}\frac{\partial\varphi_j}{\partial x}+A_{22}\left(\frac{\partial w_0}{\partial y}\right)^2\frac{\partial\varphi_j}{\partial y}+A_{26}\left(\frac{\partial w_0}{\partial x}\frac{\partial w_0}{\partial y}\frac{\partial\varphi_j}{\partial y}+\frac{\partial\varphi_j}{\partial x}\left(\frac{\partial w_0}{\partial y}\right)^2\right)\right]\right\}\right\rangle dxdy$$

$$K_{ij}^{34} = \int_{\Omega^e}\left(\frac{\partial\varphi_i}{\partial x}A_{55}\psi_j+\frac{\partial\varphi_i}{\partial y}A_{45}\psi_j\right)dxdy$$

$$(K_{NL}^{34})_{ij} = \int_{\Omega^e}\left\{\frac{\partial\psi_i}{\partial x}\left[\frac{\partial w_0}{\partial x}\left(B_{11}\frac{\partial\psi_j}{\partial x}+B_{16}\frac{\partial\psi_j}{\partial y}\right)+\frac{\partial w_0}{\partial y}\left(B_{16}\frac{\partial\psi_j}{\partial x}+B_{66}\frac{\partial\psi_j}{\partial y}\right)\right]\right.$$
$$\left.+\frac{\partial\psi_i}{\partial y}\left[\frac{\partial w_0}{\partial x}\left(B_{16}\frac{\partial\psi_j}{\partial x}+B_{66}\frac{\partial\psi_j}{\partial y}\right)+\frac{\partial w_0}{\partial y}\left(B_{12}\frac{\partial\psi_j}{\partial x}+B_{26}\frac{\partial\psi_j}{\partial y}\right)\right]\right\}dxdy$$

$$K_{ij}^{35} = \int_{\Omega^e}\left[\frac{\partial\varphi_i}{\partial x}\left(A_{45}\psi_j\right)+\frac{\partial\varphi_i}{\partial y}\left(\overline{A}_{44}\psi_j\right)\right]dxdy\,,$$

$$(K_{NL}^{35})_{ij} = \int_{\Omega^e}\left\{\frac{\partial\psi_i}{\partial x}\left[\frac{\partial w_0}{\partial x}\left(B_{12}\frac{\partial\psi_j}{\partial y}+B_{16}\frac{\partial\psi_j}{\partial x}\right)+\frac{\partial w_0}{\partial y}\left(B_{26}\frac{\partial\psi_j}{\partial y}+B_{66}\frac{\partial\psi_j}{\partial x}\right)\right]\right.$$
$$\left.+\frac{\partial\psi_i}{\partial y}\left[\frac{\partial w_0}{\partial x}\left(B_{26}\frac{\partial\psi_j}{\partial y}+B_{66}\frac{\partial\psi_j}{\partial x}\right)+\frac{\partial w_0}{\partial y}\left(B_{22}\frac{\partial\psi_j}{\partial y}+B_{26}\frac{\partial\psi_j}{\partial x}\right)\right]\right\}dxdy$$

$$K_{ij}^{41} = \int_{\Omega^e}\left[B_{11}\frac{\partial\psi_i}{\partial x}\frac{\partial\psi_j}{\partial x}+B_{66}\frac{\partial\psi_i}{\partial y}\frac{\partial\psi_j}{\partial y}+B_{16}\left(\frac{\partial\psi_i}{\partial x}\frac{\partial\psi_j}{\partial y}+\frac{\partial\psi_i}{\partial y}\frac{\partial\psi_j}{\partial x}\right)\right]dxdy\,,$$

$$K_{ij}^{42} = \int_{\Omega^e}\left(B_{12}\frac{\partial\psi_i}{\partial x}\frac{\partial\psi_j}{\partial y}+B_{16}\frac{\partial\psi_i}{\partial x}\frac{\partial\psi_j}{\partial x}+B_{26}\frac{\partial\psi_i}{\partial y}\frac{\partial\psi_j}{\partial y}+B_{66}\frac{\partial\psi_i}{\partial y}\frac{\partial\psi_j}{\partial x}\right)dxdy\,,$$

$$(K_{NL}^{43})_{ij} = \int_{\Omega^e}\left\{\frac{1}{2}\left[\left(B_{11}\frac{\partial w_0}{\partial x}\frac{\partial \psi_i}{\partial x}\frac{\partial \varphi_j}{\partial x} + B_{12}\frac{\partial w_0}{\partial y}\frac{\partial \psi_i}{\partial x}\frac{\partial \varphi_j}{\partial y} + B_{16}\left(\frac{\partial w_0}{\partial x}\frac{\partial \psi_i}{\partial x}\frac{\partial \varphi_j}{\partial y} + \frac{\partial w_0}{\partial y}\frac{\partial \psi_i}{\partial x}\frac{\partial \varphi_j}{\partial x}\right)\right)\right.\right.$$
$$\left.\left. + \left(B_{16}\frac{\partial w_0}{\partial x}\frac{\partial \psi_i}{\partial y}\frac{\partial \varphi_j}{\partial x} + B_{26}\frac{\partial w_0}{\partial y}\frac{\partial \psi_i}{\partial y}\frac{\partial \varphi_j}{\partial y} + B_{66}\left(\frac{\partial w_0}{\partial x}\frac{\partial \psi_i}{\partial y}\frac{\partial \varphi_j}{\partial y} + \frac{\partial w_0}{\partial y}\frac{\partial \psi_i}{\partial y}\frac{\partial \varphi_j}{\partial x}\right)\right)\right]\right\}dxdy$$

$$K_{ij}^{44} = \int_{\Omega^e}\left[D_{11}\frac{\partial \psi_i}{\partial x}\frac{\partial \psi_j}{\partial x} + D_{66}\frac{\partial \psi_i}{\partial y}\frac{\partial \psi_j}{\partial y} + D_{16}\left(\frac{\partial \psi_i}{\partial x}\frac{\partial \psi_j}{\partial y} + \frac{\partial \psi_i}{\partial y}\frac{\partial \psi_j}{\partial x}\right) + A_{55}\psi_i\psi_j\right]dxdy\,,$$

$$K_{ij}^{45} = \int_{\Omega^e}\left(D_{12}\frac{\partial \psi_i}{\partial x}\frac{\partial \psi_j}{\partial y} + D_{16}\frac{\partial \psi_i}{\partial x}\frac{\partial \psi_j}{\partial x} + D_{26}\frac{\partial \psi_i}{\partial y}\frac{\partial \psi_j}{\partial y} + D_{66}\frac{\partial \psi_i}{\partial y}\frac{\partial \psi_j}{\partial x} + A_{45}\psi_i\psi_j\right)dxdy\,,$$

$$K_{ij}^{51} = \int_{\Omega^e}\left(B_{16}\frac{\partial \psi_i}{\partial x}\frac{\partial \psi_j}{\partial x} + B_{66}\frac{\partial \psi_i}{\partial x}\frac{\partial \psi_j}{\partial y} + B_{12}\frac{\partial \psi_i}{\partial y}\frac{\partial \psi_j}{\partial x} + B_{26}\frac{\partial \psi_i}{\partial y}\frac{\partial \psi_j}{\partial y}\right)dxdy\,,$$

$$K_{ij}^{52} = \int_{\Omega^e}\left[B_{22}\frac{\partial \psi_i}{\partial y}\frac{\partial \psi_j}{\partial y} + B_{66}\frac{\partial \psi_i}{\partial x}\frac{\partial \psi_j}{\partial x} + B_{26}\left(\frac{\partial \psi_i}{\partial x}\frac{\partial \psi_j}{\partial y} + \frac{\partial \psi_i}{\partial y}\frac{\partial \psi_j}{\partial x}\right)\right]dxdy\,,$$

$$(K_{NL}^{53})_{ij} = \int_{\Omega^e}\left\{\frac{1}{2}\left[\left(B_{12}\frac{\partial w_0}{\partial x}\frac{\partial \psi_i}{\partial y}\frac{\partial \varphi_j}{\partial x} + B_{22}\frac{\partial w_0}{\partial y}\frac{\partial \psi_i}{\partial y}\frac{\partial \varphi_j}{\partial y} + B_{26}\left(\frac{\partial w_0}{\partial x}\frac{\partial \psi_i}{\partial y}\frac{\partial \varphi_j}{\partial y} + \frac{\partial w_0}{\partial y}\frac{\partial \psi_i}{\partial y}\frac{\partial \varphi_j}{\partial x}\right)\right)\right.\right.$$
$$\left.\left. + \left(B_{16}\frac{\partial w_0}{\partial x}\frac{\partial \psi_i}{\partial x}\frac{\partial \varphi_j}{\partial x} + B_{26}\frac{\partial w_0}{\partial y}\frac{\partial \psi_i}{\partial x}\frac{\partial \varphi_j}{\partial y} + B_{66}\left(\frac{\partial w_0}{\partial x}\frac{\partial \psi_i}{\partial x}\frac{\partial \varphi_j}{\partial y} + \frac{\partial w_0}{\partial y}\frac{\partial \psi_i}{\partial x}\frac{\partial \varphi_j}{\partial x}\right)\right)\right]\right\}dxdy$$

$$K_{ij}^{54} = \int_{\Omega^e}\left(D_{16}\frac{\partial \psi_i}{\partial x}\frac{\partial \psi_j}{\partial x} + D_{66}\frac{\partial \psi_i}{\partial x}\frac{\partial \psi_j}{\partial y} + D_{12}\frac{\partial \psi_i}{\partial y}\frac{\partial \psi_j}{\partial x} + D_{26}\frac{\partial \psi_i}{\partial y}\frac{\partial \psi_j}{\partial y}A_{45}\psi_i\psi_j\right)dxdy \quad ,$$

$$K_{ij}^{55} = \int_{\Omega^e}\left[D_{22}\frac{\partial \psi_i}{\partial y}\frac{\partial \psi_j}{\partial y} + D_{66}\frac{\partial \psi_i}{\partial x}\frac{\partial \psi_j}{\partial x} + D_{26}\left(\frac{\partial \psi_i}{\partial x}\frac{\partial \psi_j}{\partial y} + \frac{\partial \psi_i}{\partial y}\frac{\partial \psi_j}{\partial x}\right) + A_{44}\psi_i\psi_j\right]dxdy\,,$$

$$M_{ij}^{11} = \int_{\Omega^e} I_0\psi_i\psi_j dxdy\,,\quad M_{ij}^{22} = \int_{\Omega^e} I_0\psi_i\psi_j dxdy\,,\quad M_{ij}^{33} = \int_{\Omega^e} I_0\varphi_i\varphi_j dxdy\,,$$

$$M_{ij}^{44} = \int_{\Omega^e} I_2\psi_i\psi_j dxdy\,,\quad M_{ij}^{55} = \int_{\Omega^e} I_2\psi_i\psi_j dxdy\,,$$

$$C_{ij}^{13} = \int_{\Omega^e}\left\{\left[\sum_{k=1}^{N}(Z_{k+1} - Z_k)\right][e_m d_m k_c C(t)]\frac{\partial \psi_i}{\partial x}\varphi_j\right\}dxdy\,,$$

$$C_{ij}^{23} = \int_{\Omega^e}\left\{\left[\sum_{k=1}^{N}(Z_{k+1} - Z_k)\right][e_m d_m k_c C(t)]\frac{\partial \psi_i}{\partial y}\varphi_j\right\}dxdy\,,$$

$$C_{ij}^{33} = \int_{\Omega^e}\left\{c_1\left[\sum_{k=1}^{N}\frac{1}{4}\left(Z_{k+1}{}^4 - Z_k{}^4\right)\right][e_m d_m k_c C(t)]\left(\frac{\partial^2 \varphi_i}{\partial x^2} + \frac{\partial^2 \varphi_i}{\partial y^2}\right)\varphi_j\right\}dxdy\,,$$

$$C_{ij}^{43} = \int_{\Omega^e} \left\{ \left(\left[\sum_{k=1}^{N} \frac{1}{2} \left({Z_{k+1}}^2 - {Z_k}^2 \right) \right] - c_1 \left[\sum_{k=1}^{N} \frac{1}{4} \left({Z_{k+1}}^4 - {Z_k}^4 \right) \right] \right) [e_m d_m k_c C(t)] \frac{\partial \psi_i}{\partial x} \varphi_j \right\} dxdy ,$$

$$C_{ij}^{53} = \int_{\Omega^e} \left\{ \left(\left[\sum_{k=1}^{N} \frac{1}{2} \left({Z_{k+1}}^2 - {Z_k}^2 \right) \right] - c_1 \left[\sum_{k=1}^{N} \frac{1}{4} \left({Z_{k+1}}^4 - {Z_k}^4 \right) \right] \right) [e_m d_m k_c C(t)] \frac{\partial \psi_i}{\partial y} \varphi_j \right\} dxdy ,$$

$$F_i^1 = \oint_{\Gamma^e} \left(N_{xx} n_x + N_{xy} n_y \right) \psi_i ds , \quad F_i^2 = \oint_{\Gamma^e} \left(N_{xy} n_x + N_{yy} n_y \right) \psi_i ds , \quad F_i^3 = \int_{\Omega^e} q \varphi_i dxdy + \oint_{\Gamma^e} \left(V_n \varphi_i \right) ds ,$$

$$F_i^4 = \oint_{\Gamma^e} \left(M_{xx} n_x + M_{xy} n_y \right) \psi_i ds , \quad F_i^5 = \oint_{\Gamma^e} \left(M_{xy} n_x + M_{yy} n_y \right) \psi_i ds ,$$

$$F_i^{T1} = \int_{\Omega^e} \left(\frac{\partial \psi_i}{\partial x} N_{xx}^T + \frac{\partial \psi_i}{\partial y} N_{xy}^T \right) dxdy , \quad F_i^{T2} = \int_{\Omega^e} \left(\frac{\partial \psi_i}{\partial x} N_{xy}^T + \frac{\partial \psi_i}{\partial y} N_{yy}^T \right) dxdy ,$$

$$F_i^{T4} = \int_{\Omega^e} \left(\frac{\partial \psi_i}{\partial x} M_{xx}^T + \frac{\partial \psi_i}{\partial y} M_{xy}^T \right) dxdy , \quad F_i^{T5} = \int_{\Omega^e} \left(\frac{\partial \psi_i}{\partial x} M_{xy}^T + \frac{\partial \psi_i}{\partial y} M_{yy}^T \right) dxdy ,$$

$$F_i^{M1} = \int_{\Omega^e} \left(\frac{\partial \psi_i}{\partial x} N_{xx}^M + \frac{\partial \psi_i}{\partial y} N_{xy}^M \right) dxdy , \quad F_i^{M2} = \int_{\Omega^e} \left(\frac{\partial \psi_i}{\partial x} N_{xy}^M + \frac{\partial \psi_i}{\partial y} N_{yy}^M \right) dxdy ,$$

$$F_i^{M4} = \int_{\Omega^e} \left(\frac{\partial \psi_i}{\partial x} M_{xx}^M + \frac{\partial \psi_i}{\partial y} M_{xy}^M \right) dxdy , \quad F_i^{M5} = \int_{\Omega^e} \left(\frac{\partial \psi_i}{\partial x} M_{xy}^M + \frac{\partial \psi_i}{\partial y} M_{yy}^M \right) dxdy .$$